ChemPubSoc Europe

DOI: 10.1002/chem.201303853

CHEMISTRY
A European Journal
Full Paper

Yttrium Complexes

Metal-to-Ligand Alkyl Migration Inducing Carbon–Sulfur Bond Cleavage in Dialkyl Yttrium Complexes Supported by Thiazole-Containing Amidopyridinate Ligands: Synthesis, Characterization, and Catalytic Activity in the Intramolecular Hydroamination Reaction

Dmitry M. Lyubov,[a] Lapo Luconi,[b] Andrea Rossin,[b] Giulia Tuci,[b] Anton V. Cherkasov,[a] Georgy K. Fukin,[a] Giuliano Giambastiani,*[b] and Alexander A. Trifonov*[a]

Abstract: Neutral Y^{III} dialkyl complexes supported by tridentate N^-,N,N monoanionic methylthiazole– or benzothiazole–amidopyridinate ligands have been prepared and completely characterized. Studies on their stability in solution revealed progressive rearrangement of the coordination sphere in the benzothiazole-containing system through an unprecedented metal-to-ligand alkyl migration and subsequent thiazole ring opening. Attempts to synthesize hydrido species from the dialkyl precursor led to the generation of a dimeric yttrium species stabilized by a trianionic N^-,N,N^-,S^- ligand as the result of metal-to-ligand hydride migration with chemoselective thiazole ring opening and subsequent dimerization through intermolecular addition of the residual Y–H group to the imino fragment of a second equivalent of the ring-opened intermediate. DFT calculations were used to elucidate the thermodynamics and kinetics of the process, in support of the experimental evidence. Finally, all isolated yttrium complexes, especially their cationic forms prepared by activation with the Lewis acid $Ph_3C^+[B(C_6F_5)_4]^-$, were found to be good candidate catalysts for intramolecular hydroamination/cyclization reactions. Their catalytic performance with a number of primary and secondary amino alkenes was assessed.

Introduction

Rare earth metal alkyls have attracted a great deal of attention due to their unique reactivity,[1] which enables difficult reactions such as hydrocarbon activation[2] and alkane functionalization.[3] Moreover, extensive research in the past three decades has revealed the great potential of rare earth metal alkyl derivatives as catalysts (or precatalysts) of various transformations involving alkenes and alkynes, such as polymerization,[4] hydrogenation,[5] hydrosilylation,[6] hydroamination,[7] and hydroboration.[8] More recently, cationic monoalkyl rare earth metal complexes have emerged as valuable candidates for promoting catalytic homo- and copolymerization of olefins and dienes.[9]

Due to the large size of rare earth metal ions, the coordination number and steric hindrance at the metal center play a central role in controlling both their stability and chemical reactivity. Therefore, the design and synthesis of tailored ancillary ligands suitable for coordination to rare earth metal ions, isolation of the corresponding alkyl species, and investigation of their complex structure–reactivity relationships are currently one of the main trends in organo rare earth metal chemistry[10] and an essential tool for fine-tuning of the reactivity of the complexes.

We have recently described the use of bulky aminopyridinate ligands for the synthesis of a number of surprisingly thermally stable dialkyl organolanthanide complexes.[11] Modification of the ligand framework through introduction of a methylene or quaternary CMe_2 bridge between the amido and pyridine groups changes the chelate bite angle and results in derivatives with modified stability and reactivity.[12] In particular, the reaction of modified ligands with $[Y(CH_2SiMe_3)_3(thf)_2]$[13] does not yield the expected yttrium dialkyl complexes, but instead produces the monoalkyl derivatives as a result of intramolecular activation of an sp^2 or sp^3 C–H bond in the dangling substituents of the central pyridine unit.

Herein, we describe the synthesis and characterization of a new family of Y^{III} dialkyl complexes stabilized by tridentate N^-,N,N monoanionic methylthiazole– or benzothiazole–amidopyridinate ligands as well as the ability of their cationic coun-

[a] Dr. D. M. Lyubov, A. V. Cherkasov, Prof. G. K. Fukin, Prof. A. A. Trifonov
G. A. Razuvaev Institute of Organometallic Chemistry
of the Russian Academy of Sciences
Tropinina 49, GSP-445, 603950 Nizhny Novgorod (Russia)
E-mail: trif@iomc.ras.ru

[b] Dr. L. Luconi, Dr. A. Rossin, Dr. G. Tuci, Dr. G. Giambastiani
Institute of Chemistry of Organometallic Compounds
ICCOM-CNR
Via Madonna del Piano, 10, 50019 Sesto Fiorentino (Italy)
Fax: (+39) 055-5225203
E-mail: giuliano.giambastiani@iccom.cnr.it

Supporting information for this article is available on the WWW under http://dx.doi.org/10.1002/chem.201303853.

terparts to perform efficiently the catalytic intramolecular hydroamination of a variety of primary and secondary amino alkenes. An in-depth evaluation of the stability of the dialkyl species revealed the occurrence of a novel reaction path for the benzothiazole-containing complex. As a result of an alkyl migration, ring opening of the heterocycle occurs with concomitant generation of a monoalkyl aryl thiolate yttrium species stabilized by a tetradentate N^-,N,N,S^- dianionic ligand. DFT calculations were used to elucidate the thermodynamics and kinetics of the process, in support of the experimental evidence. Finally, a full account of the catalytic performance of the neutral and cationic forms of the yttrium alkyl complexes in the hydroamination of primary and secondary amino alkene substrates is given.

Results and Discussion

Synthesis of the tridentate N,N,N ligands HL^{Thia} (6a), $HL^{Thia}Me_2$ (6b), and $HL^{BnTh}Me_2$ (7)

Scheme 1 illustrates the stepwise procedure developed to prepare 5-methylthiazole- and benzothiazole-substituted aminopyridine ligands **6a**,**b** and **7** in moderate yields. Bromo intermediates **3a**,**b**, 2-(trimethylstannyl)benzothiazole (**4**), and 5-methyl-2-(trimethylstannyl)thiazole (**5**) were prepared according to literature procedures,[14,15] in some cases with slight modifications.[16] 6-Bromo-2-pyridinecarboxaldehyde (**1a**) and 2-acetyl-6-bromopyridine (**1b**) were converted to imine derivatives **2a**,**b** under classical condensation conditions in the presence of a catalytic amount of formic acid.[17] Reduction of imines **2a** and **2b** by treatment with $NaCNBH_3$/AcOH[18] or $AlMe_3$ resulted in formation of the corresponding secondary aniline derivatives **3a** and **3b**, respectively. The aminopyridine ligands HL^{Thia} (**6a**), $HL^{Thia}Me_2$ (**6b**), and $HL^{BnTh}Me_2$ (**7**) were prepared in the form of off-white crystals (60–80% yield) by Stille coupling between **3a**,**b** and **4** or **5**, respectively (see Experimental Section). In all three ligands, the donor-atom set consists of a nitrogen donor site of the electron-poor thiazole or benzothiazole framework and two hard nitrogen coordination sites from the pyridine central unit and the amido pendant arm (N^-).

Synthesis and characterization of dialkyl Y^{III} amidopyridinate complexes 8a,b and 9

The reaction of ligands **6a**,**b** with an equimolar amount of [$Y(CH_2SiMe_3)_3(thf)_2$] proceeded smoothly in toluene at 0 °C for 2 h to give dark-red solutions of the expected dialkyl compounds **8a**,**b** (Scheme 2). The reaction course was monitored by ^{1}H NMR spectroscopy, which revealed complete ligand complexation within 2 h. After cooling to −30 °C overnight, both concentrated crude mixtures give dark red, highly air and moisture sensitive crystals of complexes **8a**,**b**, which were isolated in 74 and 61% yield, respectively.

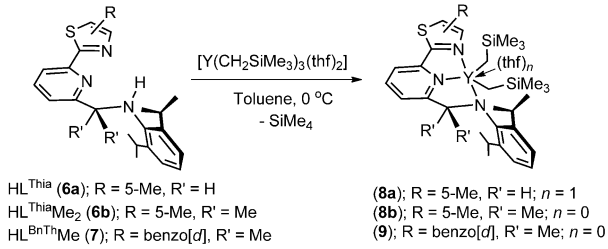

Scheme 2. Synthesis of yttrium dialkyl complexes **8a**,**b** and **9**.

Both dialkyl complexes are sparingly soluble in aliphatic hydrocarbons (*n*-pentane and hexane), but fairly soluble in THF and apolar aromatic hydrocarbons (toluene and benzene); the latter property is the main cause of the moderate yields of the precipitated solid compounds. Crystals of **8a**,**b** can be conveniently stored for months under inert atmosphere and at room temperature without any apparent decomposition. Similarly, the ^{1}H NMR spectra of both compounds in [D_6]benzene solution remained unchanged at room temperature or temperatures below solvent reflux. ^{1}H NMR and $^{13}C\{^1H\}$ NMR spectra of **8a**,**b** showed similar patterns with superimposable spectral regions. The most relevant spectral features are resonances for a pair of diastereotopic isopropyl methyl groups [two doublets at $\delta_H = 1.52/1.43$ ppm (**8a**) and $\delta_H = 1.26/1.43$ ppm (**8b**)], a $-CHMe_2$ septet [$\delta_H = 4.22$ (**8a**)/3.70 ppm (**8b**)], and a singlet resonance for the bridging PyCH_2N moiety (**8a**: $\delta_H = 4.91$ ppm). In both complexes, the methylene protons of the alkyl groups attached to yttrium are diastereotopic and appear as two doublets of doublets cen-

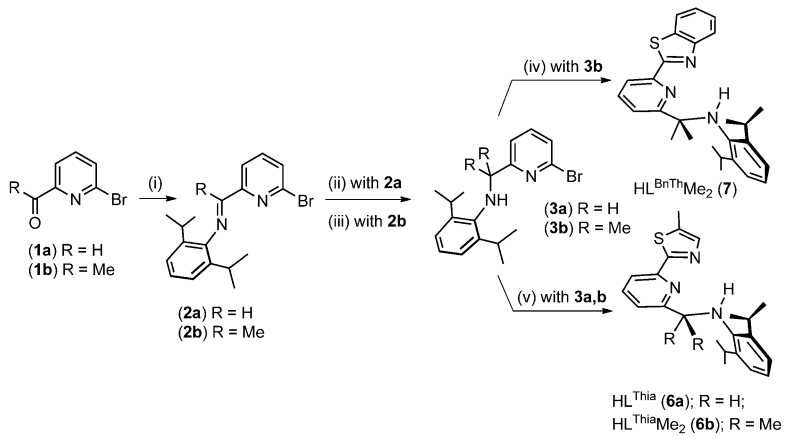

Scheme 1. Synthesis of ligands **6a**,**b** and **7**. i) 2,6-Diisopropylaniline, HCOOH cat., MeOH, reflux; ii) $NaBH_3CN$, AcOH, THF/MeOH; iii) Trimethylaluminum, toluene, 0 °C; iv) 2-(Trimethylstannyl)benzothiazole (**4**), [$Pd(dba)_2$]/PPh_3 cat., toluene, reflux; v) 5-Methyl-2-(trimethylstannyl)thiazole (**5**) [$Pd(dba)_2$]/PPh_3 cat., toluene, reflux.

tered at $\delta_H = -0.84$ (dd, $^2J_{HH} = 10.7$, $^2J_{YH} = 2.3$ Hz)/-0.67 ppm (dd, $^2J_{HH} = 10.7$, $^2J_{YH} = 2.9$ Hz) for **8a** and $\delta_H = -0.28$ (dd, $^2J_{HH} = 11.1$, $^2J_{YH} = 3.0$ Hz)/-0.16 ppm (dd, $^2J_{HH} = 11.1$, $^2J_{YH} = 3.1$ Hz) for **8b**. The respective methylene carbon atoms give rise to doublets centered at $\delta_C = 27.8$ (**8a**: d, $^1J_{YC} = 32.8$ Hz)/35.6 ppm (**8b**: d, $^1J_{YC} = 39.2$ Hz). Sharp singlets occur for the $SiMe_3$ groups in the ^1H [$\delta_H = -0.08$ (**8a**)/0.15 ppm (**8b**)] and $^{13}C\{^1H\}$ NMR spectra [$\delta_C = 3.9$ (**8a**)/4.1 ppm (**8b**)]. Finally, two broad signals in **8a**, centered at $\delta_H = 1.25$ and 3.45 ppm, were assigned to the α- and β-methylene protons of a thf ligand, respectively.

Crystals of **8a** and **8b** suitable for X-ray analysis were obtained by prolonged cooling of concentrated solutions in toluene at $-30\,^\circ C$, and their molecular structures are shown in Figures 1 and 2, respectively. Table 1 lists crystal data and structural-refinement details. Complex **8a** crystallizes in space group $P2_1/n$ with four molecules in the unit cell. The six-coordinate

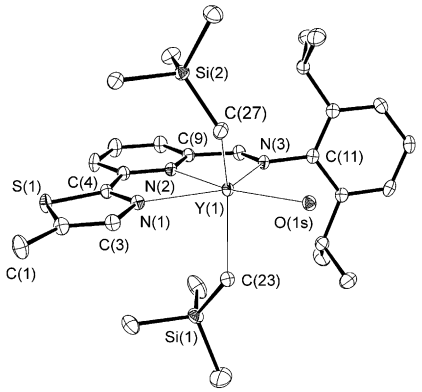

Figure 1. Crystal structure of **8a**. Thermal ellipsoids are drawn at 40% probability. Hydrogen atoms and methylene groups of the coordinated thf molecule are omitted for clarity. Selected bond lengths [Å] and angles [°]: Y(1)–N(3) 2.2717(14), Y(1)–C(23) 2.4505(18), Y(1)–C(27) 2.4522(19), Y(1)–O(1S) 2.4664(12), Y(1)–N(2) 2.4812(14), Y(1)–N(1) 2.5271(14); C(23)-Y(1)-C(27) 126.61(6), N(3)-Y(1)-N(2) 67.89(5), N(3)-Y(1)-N(1) 132.52(5), N(2)-Y(1)-N(1) 64.63(5).

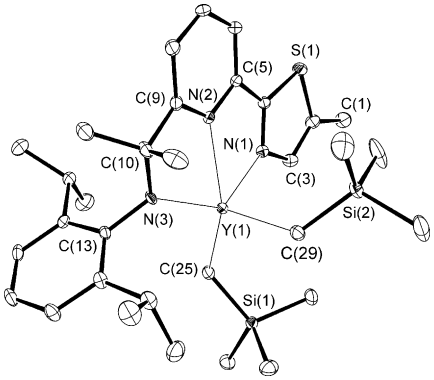

Figure 2. Crystal structure of **8b**. Thermal ellipsoids are drawn at 40% probability. Hydrogen atoms are omitted for clarity. Selected bond lengths [Å] and angles [°]: Y(1)–N(3) 2.2297(11), Y(1)–C(29) 2.3973(15), Y(1)–C(25) 2.4386(15), Y(1)–N(2) 2.4386(12), Y(1)–N(1) 2.5153(12); C(29)-Y(1)-C(25) 108.00(5), N(3)-Y(1)-N(2) 67.96(4), N(3)-Y(1)-N(1) 129.25(4), N(2)-Y(1)-N(1) 65.65(4).

yttrium atom adopts a strongly distorted octahedral geometry with three nitrogen atoms from the organic ligand and one oxygen atom from thf occupying the equatorial plane. The apical positions are occupied by two carbon atoms from the CH_2SiMe_3 substituents. As expected, only the harder N-donor sites of the methylthiazole fragment enter the coordination sphere of the metal center, whereas the softer S site points away from the yttrium center. Moreover, variable temperature ^1H NMR spectra of **8a** (-60 to $40\,^\circ C$) showed no evidence of a dynamic process associated with $Y–N^{Thia}$ dissociation and formation of a $Y–S^{Thia}$ coordination bond. The tridentate amidopyridinate ligand is nearly planar, with an average deviation of the metal center from the N(1)N(2)N(3) plane of 0.020 Å. The Y–C distances in **8a** (2.4505(18) and 2.4522(19) Å) are very similar to each other and to those in related six-coordinate yttrium dialkyl complexes.[19] The Y–N distances in **8a** are unequal: the Y(1)–N(3) (2.2717(14) Å) bond is substantially shorter than the others (Y(1)–N(2) 2.4812(14), Y(1)–N(1) 2.5271(14) Å), but lies in the range observed for related systems.[8b,12b,19f,20]

Complex **8b** crystallizes in monoclinic space group *Pn* with two molecules per unit cell. The metal center has a coordination number of five (distorted square-pyramidal coordination geometry) with the three ligand N atoms and one CH_2SiMe_3 group in the equatorial positions and the other CH_2SiMe_3 group in the axial position.[21] Unlike **8a**, complex **8b** crystallizes without coordinated thf. Moreover, while the tridentate N-donor set is nearly coplanar in **8a** with a slight average deviation of the coordinated yttrium center from the N(1)N(2)N(3) plane, in five-coordinate complex **8b** the amido nitrogen atom N(3) deviates significantly from the plane defined by the pyridine and 5-methylthiazole rings. This results in an average deviation of the yttrium ion of 0.624 Å from the N(1)N(2)N(3) plane. Decreasing the coordination number from six (**8a**) to five (**8b**) expectedly translates into shortening of the Y–C bonds (2.3973(15) and 2.4386(15) Å). As already observed for **8a**, the Y(1)–N(3) bond length in **8b** is also substantially shorter (2.2297(11) Å) than the others (Y(1)–N(1) 2.5153(12) Å, Y(1)–N(2) 2.4386(12) Å).

Dialkyl complex **9** was prepared by reaction of **7** with an equimolar amount of $[Y(CH_2SiMe_3)_3(thf)_2]$ under the same synthetic conditions as for the 5-methylthiazole-containing ligands (Scheme 2). Complex **9** precipitated from the mother liquor on standing at $-30\,^\circ C$ overnight as a dark purple crystalline solid in 75% yield. Complex **9** shows moderate solubility in THF and apolar aromatic hydrocarbons, but it is scarcely soluble in aliphatic ones. NMR spectra and microanalysis are consistent with a compound that does not contain any thf. The most relevant ^1H NMR spectral features of **9** ([D_6]benzene) are a pair of resonances for diastereotopic isopropyl methyl groups (two doublets at $\delta_H = 1.33/1.46$ ppm), a $-CHMe_2$ septet ($\delta_H = 3.86$ ppm), and two doublets of doublets centered at $\delta_H = -0.39$ (dd, $^2J_{HH} = 11.0$, $^2J_{YH} = 2.9$ Hz)/-0.22 ppm (dd, $^2J_{HH} = 11.0$, $^2J_{YH} = 2.9$ Hz, 2H, YCH_2) assigned to the diastereotopic methylene groups of the alkyl fragments bound to the yttrium center. In the $^{13}C\{^1H\}$ NMR spectrum, the alkyl CH_2 groups appear as a slightly broadened doublet at $\delta_C = 34.0$ ppm ($^1J_{YC} = 34.9$ Hz). The six methyl groups of the $SiMe_3$ moieties appear as a sharp

Table 1. Crystal data and structure refinement for complexes **8a**, **8b**, **10**, and **12**.

	8a	8b	10	12
empirical formula	$C_{34}H_{56}N_3OSSi_2Y$	$C_{32}H_{52}N_3SSi_2Y$	$C_{39}H_{60}N_3OSSi_2Y$	$C_{54}H_{64}N_6S_2Y_2\cdot(C_7H_8)_3$
M_r	699.97	655.92	764.05	1315.45
T [K]	100(2)	100(2)	100(2)	100(2)
crystal system	monoclinic	monoclinic	monoclinic	triclinic
space group	$P2_1/n$	Pn	$P2_1/n$	$P\bar{1}$
a [Å]	11.0974(5)	9.38398(16)	11.0637(7)	10.86470(10)
b [Å]	27.4753(11)	11.56576(19)	28.4816(19)	13.0408(2)
c [Å]	13.4065(6)	16.6885(3)	12.8320(9)	13.1689(2)
α [°]	90	90	90	114.1180(10)
β [°]	108.9810(10)	91.8518(15)	95.9650(10)	100.2110(10)
γ [°]	90	90	90	97.8690(10)
V [Å^3]	3865.4(3)	1810.30(5)	4021.6(5)	1629.83(4)
Z	4	2	4	1
ρ_{calcd} [g cm^{-3}]	1.203	1.203	1.262	1.340
μ [mm^{-1}]	1.653	1.758	1.594	1.884
F(000)	1488	696	1624	690
crystal size [mm]	0.42×0.31×0.15	0.50×0.40×0.20	0.30×0.20×0.10	0.40×0.20×0.20
θ range for data collection [°]	2.08–28.00	3.01–30.00	1.98–26.00	2.92–29.00
index ranges	$-14\le h\le 14$	$-13\le h\le 13$	$-13\le h\le 13$	$-14\le$ h ≤ 14
	$-36\le k\le 36$	$-16\le k\le 16$	$-35\le k\le 35$	$-17\le$ k ≤ 17
	$-17\le l\le 17$	$-23\le l\le 22$	$-15\le l\le 15$	$-17\le l\le 17$
reflns collected	38279	22045	34021	31068
independent reflns	9308	9696	7904	8646
R_{int}	0.0519	0.0297	0.0644	0.0291
completeness to θ [%]	99.7	99.8	99.9	99.8
data/restraints/parameters	9308/0/390	9696/2/375	7904/0/434	8646/12/396
GOF on F^2	1.007	1.018	1.021	1.053
final R indices [$I>2\sigma(I)$]	$R_1=0.0384$	$R_1=0.0310$	$R_1=0.0445$	$R_1=0.0303$
	$wR_2=0.0778$	$wR_2=0.0643$	$wR_2=0.0968$	$wR_2=0.0766$
R indices (all data)	$R_1=0.0641$	$R_1=0.0367$	$R_1=0.0772$	$R_1=0.0374$
	$wR_2=0.0838$	$wR_2=0.0663$	$wR_2=0.1054$	$wR_2=0.0787$
largest diff. peak/hole [e Å^3]	0.641/−0.361	0.483/−0.238	0.615/−0.366	0.595/−0.506

singlet at $\delta_H=-0.01$ ppm and $\delta_C=4.0$ ppm in the ^{1}H NMR and $^{13}C\{^1H\}$ NMR spectra, respectively.

Thiazole ring opening promoted by metal-to-ligand 1,3-migration of an alkyl group: study on an unprecedented ligand rearrangement to give a monoalkyl yttrium complex stabilized by a tetradentate, dianionic N$^-$,N,N,S$^-$ ligand

Complex **9** is a highly air and moisture sensitive compound; nonetheless, it can be stored under inert atmosphere for prolonged periods without any apparent decomposition. A solution of **9** in [D$_6$]benzene is indefinitely stable at room temperature, but the addition of exogenous THF accelerates the progressive rearrangement of the complex to give a novel yttrium thiolate complex, the identity of which was elucidated by X-ray diffraction analysis (Scheme 3).

Thus, the addition at room temperature of two equivalents of THF to the isolated dialkyl complex **9** results in its complete rearrangement to **10** over about two months. In THF/hexane (1/1) the transformation occurs faster with complete generation of **10** in one day. On heating the mixture at 50 °C the rearrangement is complete in less than 3 h (Scheme 3). Complex **10** was isolated in 70% yield as red microcrystals from a concentrated solution in THF/hexane at −30 °C. Successive crystallization procedures from concentrated THF/hexane solutions at room temperature provided red single crystals of **10** suitable for X-ray analysis.

The molecular structure of **10** is shown in Figure 3, and crystal data and structural-refinement details are listed in Table 1. Complex **10** crystallizes in space group $P2_1/n$, with four molecules in the unit cell. The yttrium center in **10** has a formal coordination number of six (distorted octahedron) with three nitrogen atoms and one sulfur atom of a tetradentate dianionic amidothiolate ligand, an alkyl group, and one oxygen atom of a thf ligand. The novel metal coordination sphere is the result of a ligand rearrangement with generation of a tetradentate N$^-$,N,N,S$^-$ dianionic system, owing to a formal 1,3-migration of one alkyl group from the metal center to the quaternary *ipso* carbon atom of the benzothiazole group, which leads to a simultaneous opening of the heteroaromatic ring (through C–S bond cleavage) and formation

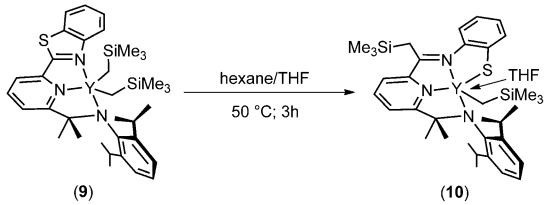

(**9**) (**10**)

Scheme 3. Metal-to-ligand alkyl migration and benzothiazole ring opening to give the yttrium thiolate complex **10**.

of a covalent Y–S bond. The Y–S bond of **10** (2.7843(8) Å) is considerably longer than those in related six-coordinate tristhiolato yttrium complexes [{(Et$_3$CS)$_2$Y(μ-SCEt$_3$)Py$_2$}$_2$] (2.642(3)–2.687(3) Å),[22a] but shorter than bridging covalent Y–S bonds in dimeric complexes [{(Et$_3$CS)$_2$Y(μ-SCEt$_3$)Py$_2$}$_2$] (2.825(3)–2.870(3) Å)[22a] and [{(Me$_3$Si)$_2$NC(NCy)$_2$}$_2$Y(μ-SnBu)]$_2$ (2.831(3), 2.804(3) Å[22b]). The Y(1)–N(1) bond (2.227(2) Å) is shorter than the Y(1)–N(3) and Y(1)–N(2) bonds (2.485(2) and 2.421(2) Å, respectively), in line with its covalent character.[23] Notably, the N(3)–C(21) bond originating from thiazole ring opening maintains the character of a C=N bond (N(3)–C(21) 1.285(4) Å) and N(3) is bound to yttrium through a coordinative interaction (Y(1)–N(3) 2.485(2) Å).[19a,23d,24] The distance between the yttrium atom and the nitrogen atom of the pyridine ring is characteristic of a coordinative Y–N bond (Y(1)–N(2) 2.421(2) Å),[24]

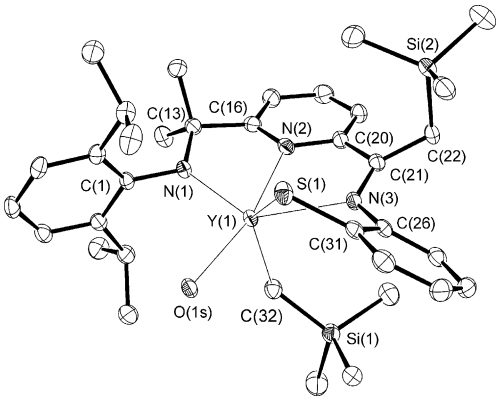

Figure 3. Crystal structure of **10**. Thermal ellipsoids are drawn at 40% probability. Hydrogen atoms and methylene groups of the coordinated thf molecule are omitted for clarity. Selected bond lengths [Å] and angles [°]: Y(1)–N(1) 2.227(2), Y(1)–O(1) 2.3970(19), Y(1)–C(32) 2.408(3), Y(1)–N(2) 2.421(2), Y(1)–N(3) 2.485(2), Y(1)–S(1) 2.7843(8), N(3)–C(21) 1.285(4), C(21)–C(22) 1.489(4); N(1)-Y(1)-N(2) 68.09(8), N(1)-Y(1)-N(3) 131.89(8), N(2)-Y(1)-N(3) 64.93(8), N(1)-Y(1)-S(1) 119.45(6), O(1)-Y(1)-S(1) 81.54(5), C(32)-Y(1)-S(1) 133.81(8), N(2)-Y(1)-S(1) 107.99(6), N(3)-Y(1)-S(1) 68.00(6).

and the Y–C bond length of the residual alkyl group (2.408(3) Å) is similar to those previously reported for six-coordinate monoalkyl yttrium complexes.[19,23] Finally, the 1,3-migration of one alkyl group to the *ipso* carbon atom of the thiazole framework results in the formation of a C–C single bond (C(21)–C(22) 1.489(4) Å).[25]

Complex **10** is highly soluble in aromatic hydrocarbons and indefinitely stable at room temperature in [D_6]benzene solution. Its most relevant ^{1}H NMR spectral features consist of two doublets of doublets centered at $\delta_H = -0.77$ and -0.74 ppm ($^2J_{HH} = 10.5$ Hz, $^2J_{YH} = 3.0$ Hz) for the residual alkyl group bound to the metal center and two doublets at $\delta_H = 2.03$ and 2.95 ppm ($^2J_{HH} = 12.5$ Hz) for the diastereotopic methylene protons of the migrated CH_2SiMe_3 group; the corresponding $SiMe_3$ protons appear as sharp singlets at $\delta_H = 0.06$ and -0.21 ppm, respectively.

Whereas there have been several reports of pyridine-based ligands undergoing further rearrangements on coordination to transition metals[26] or rare earth metals,[27] to the best of our knowledge this is a unique example of quantitative thiazole ring opening proceeding through chemoselective C–S bond cleavage while keeping the imino moiety derived from the thiazole core intact. Indeed, metal-to-ligand alkyl migrations in rare earth metal complexes are known to promote the transformation of neutral N donors into anionic amide ligands, including processes in which such a migration is associated with partial ligand dearomatization.[28] In the case of the yttrium-coordinated benzothiazole system, the electronic requirements of the electron-poor rare earth metal ion are assumed to drive the process towards the generation of a sterically and electronically saturated system that favors selective thiazole ring opening and the generation of a tetradentate dianionic chelating ligand while preserving the C=N imino group from reduction. Notably, complexes **8a**,**b** do not undergo similar rearrangement even when they are heated at 50 °C for several hours in THF/hexane. To gain additional insight into this reaction, DFT calculations were performed on model systems with the aim of elucidating the thermodynamics and kinetics of the process.

DFT modeling of the 1,3-alkyl migration and rearrangement of the complex

Density functional calculations carried out on simplified model systems at the M06/6-31G* level of theory (THF/hexane, SMD continuum model) contributed to better understanding of the process (Scheme 4). After a preliminary assessment of the energy profiles associated with the 1,3-alkyl migration and subsequent ligand rearrangement in the models, selected profiles of interest were also evaluated on the real system for the sake of completeness. Starting geometries for computational models **9a** and **9b** were obtained from the crystal structure of **8b** by replacing the N-coordinated 5-methylthiazole with an N- (**9a**) or S-coordinated (**9b**) benzothiazole group and replacing both the 2,6-*i*Pr(C_6H_3) substituent of the amido fragment and the methyl groups of the -CH_2SiMe_3 substituents with H atoms before reoptimizing the resulting structures (see also Experimental Section). Transfer of a CH_2SiH_3 group from the metal center to the *ipso* carbon atom of the benzothiazole ring was then analyzed theoretically for both **9a** and **9b**. The processes examined are summarized in Scheme 4, and the calculated relative Gibbs energies in THF/*n*-hexane (1/1)[29] are shown in Figure 4, together with the optimized geometries for reactants, transition states, and products.

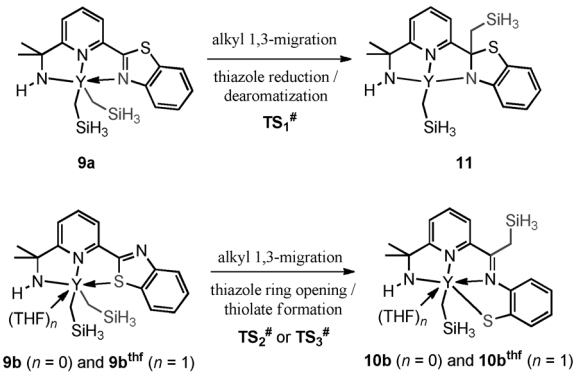

Scheme 4. Reaction processes analyzed by DFT modeling in this work.

Benzothiazole N coordination is much more stabilizing than S coordination ($\Delta G = 14.7$ kcal mol^{-1}), and σ(Si–H)···Y agostic interactions are present in **9a** (optimized *d*(Si···Y) = 3.35, *d*(Si–H···Y) = 3.10 Å), probably as a consequence of the $SiMe_3 \rightarrow SiH_3$ change on going from the real system to the DFT model. Whereas the N-coordinated ligand has approximately planar geometry (optimized N^{Py}-C-C-N^{Th} dihedral angle 5.1°), in the case of S coordination the organic fragment is far from planarity (optimized N^{Py}-C-C-S dihedral angle 22.1°); the coordination number is five for both complexes. While the coordination geometry of **9a** can be considered to be (distorted) trigonal-bipyramidal, that of **9b** is closer to square-pyramidal.

As shown in Figure 4 (upper panel), the 1,3-migration of a CH_2SiH_3 group to the *ipso* carbon atom of the benzothiazole framework does not result in the observed ring opening but

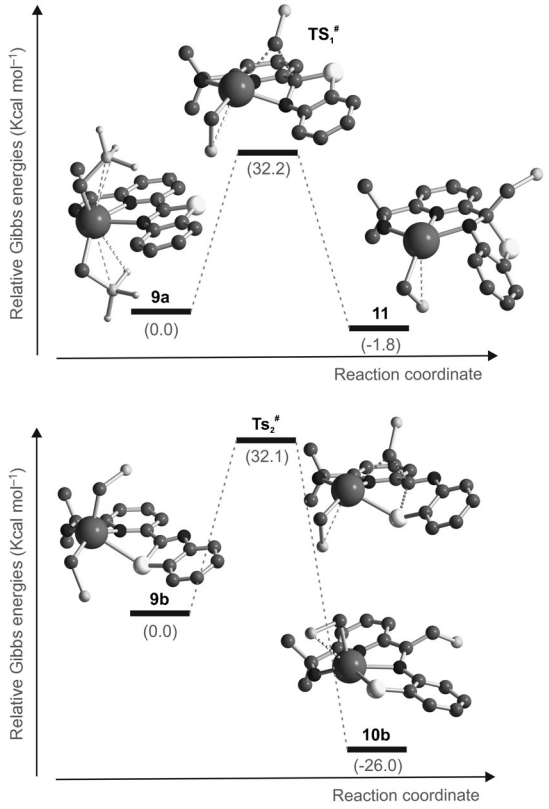

Figure 4. Gibbs energies versus reaction coordinate profiles for the two competing processes in the 1,3-migration of an alkyl fragment to the *ipso* carbon atom of the benzothiazole group. Upper panel: 1,3-Alkyl migration in **9a** and thiazole reduction/dearomatization. Lower panel: 1,3-Alkyl migration in **9b** and thiazole ring opening/thiolate formation. Optimized geometries of reactants, transition states, and products with selected bond lengths are reported in the Supporting Information.

instead induces benzothiazole reduction/dearomatization with formal generation of an anionic benzothiazoline ligand coordinated to the metal center. The *ipso* carbon atom changes its hybridization from sp^2 to sp^3 (optimized $d(C–N^{BnTh}) = 1.44$ Å in **9a**; $d(C–N^{BnTh}) = 1.31$ Å in **11**), and the more basic nature of the N donor is mirrored in a shorter Y–N distance in **11** compared to **9a** (optimized $d(Y–N) = 2.51$ Å in **9a**; $d(Y–N) = 2.26$ Å in **11**). A transition state $\mathbf{TS_1}^{\#}$ for the process was found at 32.2 kcal mol^{-1} above the reactant (Figure 4, upper panel) and the complex conversion occurs almost thermoneutrally with the product **11** lying 1.8 kcal mol^{-1} below reactant **9a**. As a result, the process is very unlikely to occur, especially from a kinetic point of view.

In the case of **9b**, migration of the CH_2SiH_3 substituent takes place with simultaneous benzothiazole ring opening through chemoselective C–S bond cleavage and generation of a benzothiolate ligand on yttrium (Scheme 4 and Figure 4, lower panel). The basic nature of the benzothiolate substituent is confirmed by the shorter Y–S distance in **10b** compared with **9b** (optimized $d(Y–S^{BnTh}) = 2.70$ Å in **10b**; $d(Y–S^{BnTh}) = 3.03$ Å in **9b**). The nitrogen atom coming from the thiazole ring is also coordinated to the metal center at the end of the CH_2SiH_3 transfer; the presence of an imino group is confirmed by the optimized $d(C=N)$ bond length of 1.30 Å. This double coordination is the thermodynamic driving force for the process to occur; in fact, although the energy barrier to be overcome is almost identical to that of the previous case ($\Delta G^{\#} = 32.1$ kcal mol^{-1} to reach $\mathbf{TS_2}^{\#}$, Figure 4, lower panel), the thermodynamics is much more downhill ($\Delta G(\mathbf{9b}–\mathbf{10b}) = -26$ kcal mol^{-1}). The comparison between the benzothiazole and the 5-methylthiazole (model) systems in the CH_2SiH_3 migration reaction (starting from the κ-S-thiazole isomer, analogous to **9b**) revealed that no ring opening takes place when the simpler 5-methylthiazole substituent is present, in line with the experimental outcome. Accordingly, the transition state corresponding to $\mathbf{TS_2}^{\#}$ could not be found on the potential-energy surface.[30]

Experiments revealed that benzothiazole ring opening occurs faster in the presence of THF as cosolvent. Accordingly, the effect of the presence of a coordinated thf molecule in the computational model was analyzed, to calculate the variation in the kinetic and thermodynamic parameters with respect to the above case, in which no thf was included in the model. Reactant **9b** was therefore modified by the addition of one thf molecule coordinated to yttrium, and the new ensemble $\mathbf{9b}^{thf}$ reoptimized. As in **9b**, the ligand in $\mathbf{9b}^{thf}$ is nonplanar (optimized N^{Py}-C-C-S dihedral angle 30.7°), the Y–S bond in $\mathbf{9b}^{thf}$ is slightly longer ($d(Y–S) = 3.03$ Å in **9b** versus 3.12 Å in $\mathbf{9b}^{thf}$), and the new coordination number is six (distorted octahedral).

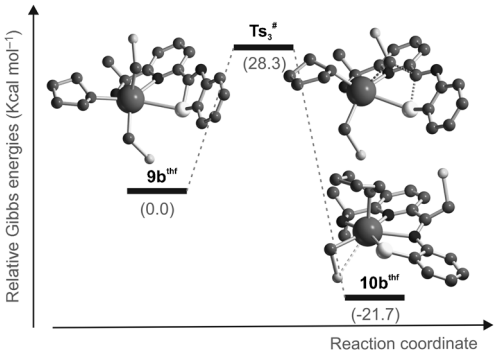

Figure 5. Gibbs energies versus reaction coordinate profiles for the 1,3-migration of an alkyl group to the *ipso* carbon atom of the benzothiazole group in complex $\mathbf{9b}^{thf}$. Optimized geometries of reactant, transition state, and product with selected bond lengths are reported in the Supporting Information.

As shown in Figure 5, the transition state ($\mathbf{TS_3}^{\#}$) lies 28.3 kcal mol^{-1} above the reactant and the calculated thermodynamics leading to $\mathbf{10b}^{thf}$ is still strongly favored ($\Delta G(\mathbf{9b}^{thf}–\mathbf{10b}^{thf}) = -21.7$ kcal mol^{-1}). The presence of a coordinated thf molecule lowers the activation barrier to be overcome, in line with the experimental findings. All of these theoretical data are in line with the experiments, in which the thiolate species was the only isolated product.

Alkyl versus hydride metal-to-ligand migration study

To further study the unprecedented reactivity observed for dialkyl complex **9**, the corresponding yttrium hydrido complex

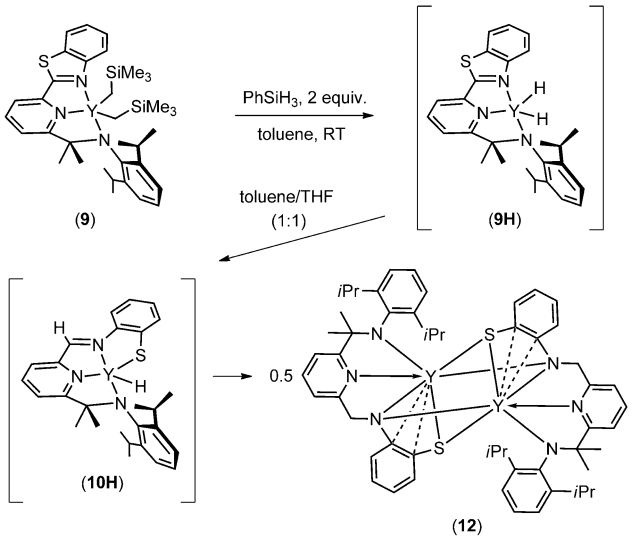

Scheme 5. Metal-to-ligand hydride migration and benzothiazole ring opening to afford dimeric complex **12**.

was synthesized by reaction of **9** with phenylsilane (Scheme 5).[12a,31] Treating a solution of complex **9** in toluene with two equivalents of $PhSiH_3$ at room temperature afforded, after solvent evaporation, a crude crystalline product, slow crystallization of which from toluene/THF (1/1) gave yellow microcrystals suitable for an X-ray diffraction study, which identified rare dimeric yttrium complex **12** (Figure 6). Crystal data and structural-refinement details are listed in Table 1.

Complex **12** crystallizes in space group $P\bar{1}$ as a toluene solvate (1.5 molecules of toluene per yttrium atom; one molecule per unit cell), and it adopts a dimeric structure featuring a central rhombic Y_2S_2 core (Y–S 2.8060(3) and 2.8474(3) Å) with two

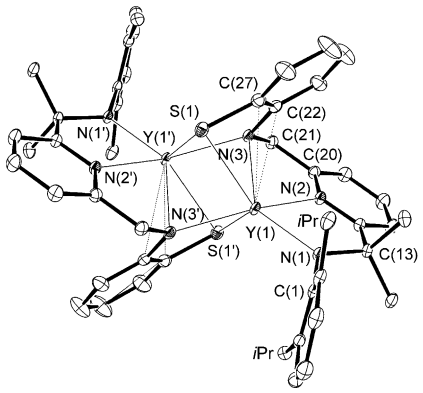

Figure 6. Crystal structure of **12**. Thermal ellipsoids are drawn at 40% probability. Hydrogen atoms, methyl groups of the *i*Pr fragments, and solvent of crystallization (toluene) are omitted for clarity. Selected bond lengths [Å] and angles [°]: Y(1)–N(1) 2.1963(8), Y(1)–N(2) 2.4019(9), Y(1)–N(3′) 2.4451(10), Y(1)–N(3) 2.4895(8), Y(1)–S(1′) 2.8060(3), Y(1)–S(1) 2.8474(3), Y(1)–C(22) 2.9253(12), Y(1)–C(27) 3.0449(12), Y(1)–Y(1′) 3.13516(18) N(3)–C(21) 1.4743(14); N(1)-Y(1)-N(2) 69.42(3), N(1)-Y(1)-N(3′) 125.06(3), N(2)-Y(1)-N(3′) 144.90(3), N(1)-Y(1)-N(3) 132.94(3), N(2)-Y(1)-N(3) 67.12(3), N(3′)-Y(1)-N(3) 101.11(3), N(1)-Y(1)-S(1′) 114.94(2), N(2)-Y(1)-S(1′) 77.58(2), N(3′)-Y(1)-S(1′) 67.32(2), N(3)-Y(1)-S(1′) 72.05(2), N(1)-Y(1)-S(1) 132.32(2), N(2)-Y(1)-S(1) 125.06(2), N(3′)-Y(1)-S(1) 71.93(2), N(3)-Y(1)-S(1) 66.10(2), S(1′)-Y(1)-S(1) 112.644(7).

nitrogen [N(3), N(3A)] and two sulfur atoms [S(1) and S(1A)] μ^2-bridging two yttrium ions [Y(1) and Y(1A)]. Thus, each Y^{3+} ion is coordinated by four nitrogen atoms and two sulfur atoms from the two bridging trianionic tetradentate N^-,N,N^-,S^- ligands with a formal coordination number of six. The Y–N bonds in **12** are nonequivalent, and the Y(1)–N(1) covalent bond is the shortest (2.1963(8) Å). Notably, the μ^2-bridging covalent bonds Y(1)–N(3) and Y(1)–N(3A) (2.4451(10) and 2.4895(8) Å) are markedly longer than the coordinative ones (Y(1)–N(2) and Y(1A)–N(2A) 2.4019(9) Å). The bond length between N(3) and the neighboring carbon atom C(21) bridging the pyridine framework (N(3)–C(21) 1.4743(14) Å) is much longer compared with the related bond length in **10** (N(3)–C(21) 1.285(4) Å); this indicates single-bond character of the C–N bond.[25] Finally, a close η^2 contact between each yttrium center and the phenyl moiety of the aryl thiolate group (*ipso*- and *ortho*-C atoms) was also found (Y(1)-C(22) 2.9253(12) and Y(1)–C(27) 3.0449(12) Å; Y(1A)–C(22A) 2.925(1) and Y(1A)–C(27A) 3.045(1) Å).

On the basis of the observed reactivity and the above-described metal-to-ligand alkyl migration, generation of the dimeric yttrium species stabilized by a trianionic N^-,N,N^-,S^- ligand is assumed to be the result of the reaction sequence summarized in Scheme 5. Firstly, treatment of **9** with two equivalents of $PhSiH_3$ results in the formation of dihydrido yttrium intermediate **9H** as the product of a σ-bond metathesis reaction.[19e,d,32] Similarly to the rearrangement described above for **9**, a metal-to-ligand 1,3-hydrido migration takes place already at room temperature with simultaneous promotion of chemoselective thiazole ring opening and generation of intermediate **10H**. Finally, the latter is expected to rapidly and quantitatively undergo intermolecular addition of the residual Y–H group to the imino fragment of a second equivalent of **10H** to generate dimeric species **12**.

Neutral and cationic yttrium complexes in the intramolecular hydroamination of amino alkenes

Organolanthanide complexes are active catalysts for the intramolecular hydroamination of both alkynes and alkenes, as pioneered by Marks and co-workers with cyclopentadienyl complexes.[7a,33] Since then, a number of group 3 organometallics (including non-cyclopentadienyl-based systems) have been extensively used as catalysts for these reactions (in both stereoselective and nonstereoselective fashion) and generally provide high turnover frequencies and, where applicable, good to excellent stereoselectivities.[7,34] Intermolecular hydroamination reactions[34a,b,m] with these catalysts are generally problematic, and most reactions catalyzed by rare earth metal complexes have been performed in an intramolecular fashion to produce predominantly pyrrolidine and piperidine derivatives.

The mechanism of hydroamination/cyclization[33c,35] classically proceeds through formation of a metal amido species with the protonolysis of a metal–alkyl bond in the precatalyst, followed by insertion of the olefin into the metal–amido bond (rate-determining step)[30b] via a seven-membered chairlike transition state (Scheme 6, for $n=1$). The resulting intermedi-

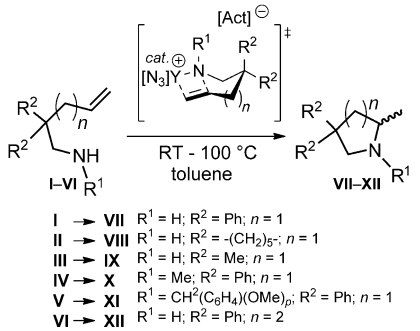

Scheme 6. Intramolecular hydroamination of primary and secondary amino alkenes.

ate undergoes fast protonolysis with a second amine molecule, which regenerates the metal amido species and releases the heterocyclic product.

In this regard, all isolated neutral alkyl compounds (**8a**,**b**, **9**, and **10**) and their cationic monoalkyl counterparts, prepared in situ, were tested as catalysts for the intramolecular hydroamination/cyclization of primary and secondary amines tethered to monosubstituted alkenes (Scheme 6, Table 2). Substrate conversions were determined by ^{1}H NMR spectroscopy with ferrocene as internal standard and confirmed by gas chromatography of the final crude reaction mixture (see Experimental Section). Details of the catalytic reactions and optimized cyclization conditions are listed in Table 2.

Cationic monoalkyl compounds were simply prepared from the respective alkyl precursors by addition of an equimolar amount of the Lewis acid $[Ph_3C][B(C_6F_5)_4]$ as an alkyl abstractor (see Experimental Section). Apparently, all cationic monoalkyl species show significantly higher catalytic activities than their neutral dialkyl analogues (Table 2, entries 1 versus 2, 5 versus 6, and 20 versus 21). This remarkable difference in reactivity is reasonably ascribed to the occurrence of stereo-electronic factors in which the nature of the monoanionic tridentate ancillary ligand plays a crucial role.[36] In contrast to the neutral complexes, the higher activity of the cationic systems reflects the beneficial effect of an additional available coordination space at the more electron deficient metal center.[37]

The cationic systems resulting from the in situ activation of **8b** and **9** are active catalysts for the intramolecular hydroamination reaction of a number of model primary and secondary amino alkenes and provide relatively fast and complete substrate conversions under relatively mild reaction conditions (from RT to 40 °C with 5 mol% of catalyst; Table 2, entries 6 and 7).

Notably, complex **8a** is the least active catalyst and shows low substrate conversions compared to analogue **8b**, even under harsher reaction conditions (Table 2, entries 3 versus 4 and 14 versus 15). This lower reactivity is ascribed to the incorporation of solvent (Lewis-base complexation) in the coordination sphere of the metal center.[9q] Indeed the thf ligand in **8a** is expected to influence the catalytic activity of the complex dramatically, owing to its electron-donating nature; hence, thf-free complex **8b** shows higher catalytic activity than thf-solvated **8a**. Comparing the two parent solvent-free complexes **8b** and **9** under similar reaction conditions (Table 2, entries 1 versus 5, 2 versus 7, 14 versus 16, 21 versus 23, 24 versus 25, and 26 versus 27) reveals that these two systems behave similarly in both their neutral and cationic forms, and the monoalkyl cationic derivative of **9** is the most catalytically active form for all selected runs. The isolated monoalkyl complex **10** shows very moderate catalytic activity when employed as it is (Table 2, entries 10 and 11), and its cationic counterpart is, as expected, totally inactive (Table 2, entries 12 and 13).

Dependence of the cyclization rate on the substrate was observed on comparing different cyclization precursors. Thus, a major kinetic Thorpe–Ingold effect in diphenyl- and cyclohexyl-substituted precursors **I** and **II** translates into almost quantitative cyclization in short reaction times to give **VII** and **VIII**, respectively (Table 2, entries 6, 7, and 17). All other scrutinized cyclization precursors (**III–VI**) typically require more severe reaction conditions (higher reaction temperature and prolonged reaction time) to give appreciable substrate conversions. Furthermore, cyclization of primary amino alkenes (generally) proceeds more efficiently than that of secondary ones (Table 2, entries 3 versus 21 and 24, 7 versus 22, and 9 versus 23 and 25).

Table 2. Intramolecular hydroamination of primary and secondary amino alkenes catalyzed by dialkyl neutral and monoalkyl cationic yttrium complexes.[a]

Entry	Catalyst	Activator	Substrate	Product	T [°C]	t [h]	Conv. [%][b]
1	**8b**	–	**I**	**VII**	40	1.5	11
2[c]	**8b**	$[Ph_3C][B(C_6F_5)_4]$	**I**	**VII**	40	1.5	97
3[c]	**8b**	$[Ph_3C][B(C_6F_5)_4]$	**I**	**VII**	80	0.75	96
4[c]	**8a**	$[Ph_3C][B(C_6F_5)_4]$	**I**	**VII**	80	2	10
5	**9**	–	**I**	**VII**	80	7	30
6[c]	**9**	$[Ph_3C][B(C_6F_5)_4]$	**I**	**VII**	RT[d]	24	98
7[c]	**9**	$[Ph_3C][B(C_6F_5)_4]$	**I**	**VII**	40	1.5	>99
8[c,e]	**9**	$[Ph_3C][B(C_6F_5)_4]$	**I**	**VII**	40	24	54
9[c]	**9**	$[Ph_3C][B(C_6F_5)_4]$	**I**	**VII**	80	0.75	>99
10	**10**	–	**I**	**VII**	40	24	18
11	**10**	–	**I**	**VII**	80	7	23
12[c]	**10**	$[Ph_3C][B(C_6F_5)_4]$	**I**	**VII**	80	0.75	–[f]
13[c]	**10**	$[Ph_3C][B(C_6F_5)_4]$	**I**	**VII**	80	24	–[f]
14[c]	**8b**	$[Ph_3C][B(C_6F_5)_4]$	**II**	**VIII**	40	2	81
15[c]	**8a**	$[Ph_3C][B(C_6F_5)_4]$	**II**	**VIII**	80	2	5
16[c]	**9**	$[Ph_3C][B(C_6F_5)_4]$	**II**	**VIII**	40	2	94
17[c]	**9**	$[Ph_3C][B(C_6F_5)_4]$	**II**	**VIII**	80	0.75	>99
18[c]	**9**	$[Ph_3C][B(C_6F_5)_4]$	**III**	**IX**	40	4	10
19[c]	**9**	$[Ph_3C][B(C_6F_5)_4]$	**III**	**IX**	80	20	36
20	**8b**	–	**IV**	**X**	80	7	–[f]
21[c]	**8b**	$[Ph_3C][B(C_6F_5)_4]$	**IV**	**X**	80	7	92
22[c]	**9**	$[Ph_3C][B(C_6F_5)_4]$	**IV**	**X**	40	4	27
23[c]	**9**	$[Ph_3C][B(C_6F_5)_4]$	**IV**	**X**	80	4	94
24[c]	**8b**	$[Ph_3C][B(C_6F_5)_4]$	**V**	**XI**	80	24	31
25[c]	**9**	$[Ph_3C][B(C_6F_5)_4]$	**V**	**XI**	80	24	92
26[c]	**8b**	$[Ph_3C][B(C_6F_5)_4]$	**VI**	**XII**	80	5	28
27[c]	**9**	$[Ph_3C][B(C_6F_5)_4]$	**VI**	**XII**	80	3	46

[a] Reaction conditions: substrate: 0.21 mmol, catalyst: 5 mol% (10.5 μmol), solvent: toluene (2.5 mL). [b] Determined by in situ ^{1}H NMR spectroscopy with ferrocene as internal standard. [c] Cationic complexes were generated in situ from the respective neutral counterparts (**8a**,**b**, **9** and **10**), as described in the Experimental Section. [d] RT: 21–22 °C. [e] Catalyst: 3 mol%. [f] No detectable amounts of cyclization products are observed.

Conclusion

We have provided a full account of the unprecedented reactivity of a class of neutral ytrrium dialkyl and dihydride complexes supported by thiazole-containing amidopyridinate ligands. In the case of the benzothiazole-containing ligand, progressive rearrangement of the coordination sphere of the yttrium dialkyl complex takes place through a metal-to-ligand 1,3-alkyl migration with subsequent chemoselective opening of the thiazole ring. The resulting monoalkyl aryl thiolate yttrium complex supported by a tetradentate N^-,N,N,S^- dianionic ligand was isolated and completely characterized in solution and in the solid state. While there have been several reports of pyridine-based ligands undergoing further rearrangements on coordination to transition metal or rare earth ions, to the best of our knowledge this is a unique example of a quantitative thiazole ring opening proceeding through chemoselective C–S bond cleavage while keeping the imino moiety derived from the thiazole core untouched. Density functional calculations on model yttrium dialkyl systems were performed to elucidate the thermodynamics and kinetics of the process, in support of the experimental evidence. Similarly, attempts to synthesize a dihydrido species from the corresponding dialkyl precursor led to the generation of an unique dimeric yttrium complex stabilized by a trianionic N^-,N,N^-,S^- ligand as the result of metal-to-ligand hydride migration, chemoselective thiazole ring opening, and subsequent dimerization of the complex by intermolecular addition of the residual YH group to the imino fragment of a second equivalent of the monohydrido yttrium intermediate. Neutral and cationic thiazole-containing yttrium alkyl complexes promote the intramolecular hydroamination of primary and secondary amino alkenes at moderate catalyst loadings (5 mol%) under relatively mild (time and temperature) reaction conditions. Other organolanthanide complexes (Lu, Yb, and Eu) supported by analogous thiazole– and benzothiazole–amidopyridinate ligands are currently under investigation as effective precatalysts for diene polymerization.

Experimental Section

General considerations and materials characterization

All air- and/or moisture-sensitive reactions were performed under inert atmosphere in flame-dried flasks by using standard Schlenk-type techniques or in a dry box filled with nitrogen. THF was purified by distillation from sodium/benzophenone ketyl after drying over KOH. Benzene, *n*-hexane, and toluene were purified by distillation from sodium/triglyme/benzophenone ketyl or by means of a MBraun solvent purification system. [D_6]Benzene was dried over sodium/benzophenone ketyl and condensed in vacuo over activated 4 Å molecular sieves prior to use, and CD_2Cl_2 was dried over activated 4 Å molecular sieves. All other reagents and solvents were used as purchased from commercial suppliers. ^{1}H and ^{13}C{^{1}H} NMR spectra were obtained on a Bruker Avance DRX-400 (400.13 and 100.62 MHz, respectively) or a Bruker Avance 300 MHz instrument (300.13 and 75.47 MHz for ^{1}H and ^{13}C, respectively). Chemical shifts δ are reported relative to TMS, referenced to the chemical shifts of residual solvent resonances (^{1}H and ^{13}C). IR spectra were recorded as Nujol mulls or KBr plates on FSM 1201 and Bruker-Vertex 70 instruments. Yttrium analysis were carried out by complexometric titration. The N, C, H elemental analyses were carried out in the microanalytical laboratory of the IOMC or at the ICCOM by means of a Carlo Erba Model 1106 elemental analyzer with an accepted tolerance of 0.4 units on C, H, and N. Melting points were determined by using a Stuart Scientific SMP3 melting point apparatus. GC analyses were performed on a Shimadzu GC-17 gas chromatograph equipped with a flame ionization detector and a Supelco SPB-1 fused silica capillary column (30 m length, 0.25 mm i.d., 0.25 μm film thickness) or a HP-PLOT Al_2O_3 KCl column (50 m length, 0.53 mm i.d., 15 μm film thickness). The GC-MS analyses were performed on a Shimadzu QP2010S apparatus equipped with a column identical to that used for GC analysis.

X-ray diffraction data

X-ray diffraction intensity data for compounds **8a**, **8b**, **10**, and **12** were collected with Bruker SMART APEX (**8a**, **8b**) and Agilent Xcalibur E (**10**, **12**) diffractometers with graphite-monochromated $Mo_{K\alpha}$ radiation ($\lambda = 0.71073$ Å) by using ω scans. The structures were solved by direct methods and were refined on F^2 by using the SHELXTL (G. M. Sheldrick, SHELXTL v.6.12, Structure Determination Software Suite, Bruker AXS, Madison, Wisconsin, USA, 2000) and Crysalis Pro [CrysAlis Pro, Agilent Technologies Ltd, Yarnton, England, 2011) software packages. All non-hydrogen atoms were located from Fourier syntheses of electron density and were refined anisotropically. All hydrogen atoms were placed in calculated positions and were refined in the riding model. SADABS (G. M. Sheldrick, SADABS v.2.01, Bruker/Siemens Area Detector Absorption Correction Program, Bruker AXS, Madison, Wisconsin, USA, 1998) and ABSPACK (Crysalis Pro) were used to perform area-detector scaling and absorption corrections. Crystallographic, collection, and refinement data are listed in Table 1, and corresponding cif files are available as supporting information. Molecular plots were produced by the program ORTEP3.[38] CCDC 962956 (**8a**), 962957 (**8b**), 962958 (**10**) and 962959 (**12**) contain the supplementary crystallographic data for this paper. These data can be obtained free of charge from The Cambridge Crystallographic Data Centre via ccdc.cam.ac.uk/products/csd/request.

Synthesis of HL^{Thia} (6a)

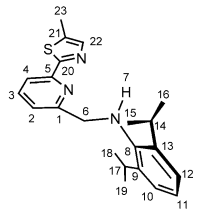

A solution of **3a** (1.00 g, 2.9 mmol) and 5-methyl-2-(trimethylstannyl)-thiazole (**5**; 1.14 g, 4.3 mmol) in dry and degassed toluene (10 mL) was treated with a solution of [Pd(dba)$_2$] (dba = *trans*,*trans*-dibenzylideneacetone; 0.050 g, 0.09 mmol) and PPh_3 (0.182 g, 0.69 mmol) in toluene (5 mL). The reaction mixture was heated to reflux for 20 h, cooled to room temperature, and treated with water (15 mL). The resulting layers were separated, and the aqueous phase was extracted with AcOEt (3×10 mL) and dried over Na_2SO_4. The collected organic layers were evaporated under reduced pressure to give the crude product. The product was purified by recrystallization from hot MeOH by cooling the resulting solution at −20 °C overnight to afford white needle crystals (0.79 g, 75.0% yield). ^{1}H NMR (400 MHz, CD_2Cl_2, 293 K): $\delta = 1.31$ (d, $^3J_{HH} = 6.8$ Hz, 12H, CH(CH_3), H^{15,16,18,19}), 2.58 (s, 3H, H^{23}), 3.54 (sept, $^3J_{HH} = 6.8$ Hz, 2H, C*H*(CH$_3$), H^{14,17}), 4.25 (s, 2H, H^6), 7.09 (m, 1H, CH Ar, H^{11}), 7.15–7.17 (2H, CH Ar, H^{10,12}), 7.32 (d, $^3J_{HH} = 7.7$ Hz, 1H, CH Ar, H^2), 7.61 (m, 1H, CH thiazole, H^{22}), 7.79 (t, $^3J_{HH} = 7.7$ Hz, 1H, CH Ar, H^3), 8.07 ppm (d, $^3J_{HH} =$

7.7 Hz, 1H, CH Ar, H^4); $^{13}C\{^1H\}$ NMR (100 MHz, CD_2Cl_2, 293 K): $\delta =$ 11.9 (C^{23}), 24.0 ($CH(CH_3)_2$, $C^{15,16,18,19}$), 27.7 ($CH(CH_3)_2$, $C^{14,17}$), 55.9 (CH_2NH, C^6), 117.3 (C^4), 122.3 (C^2), 123.4 ($C^{10,12}$), 123.7 (C^{11}), 136.7 (C), 137.4 (C^3), 141.9 (C^{22}), 142.6 (C), 143.5 (C), 151.4 (C), 158.5 (C), 167.3 ppm (C); elemental analysis calcd (%) for $C_{27}H_{31}N_3S$ (365.53 g mol^{-1}): C 72.29, H 7.45, N 11.50, S 8.77; found: C 72.40, H 7.65, N 11.45, S 8.50.

Synthesis of $HL^{Thia}Me_2$ (6b)

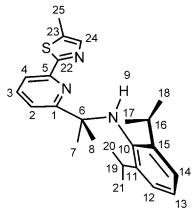

A solution of **3b** (1.00 g, 2.6 mmol) and 5-methyl-2-(trimethylstannyl)thiazole (**5**; 1.05 g, 4.0 mmol) in dry and degassed toluene (10 mL) was treated with a solution of $[Pd(dba)_2]$ (0.045 g, 0.08 mmol) and PPh_3 (0.163 g, 0.62 mmol) in toluene (5 mL). The reaction mixture was heated to reflux for 20 h, cooled to room temperature, and treated with water (15 mL). The resulting layers were separated; the aqueous phase was extracted with AcOEt (3×10 mL) and then dried over Na_2SO_4. The collected organic layers were evaporated under reduced pressure to give a crude product. The product was purified by recrystallization from hot MeOH by cooling the resulting solution at −20 °C overnight to afford white crystals (0.82 g, 80.0% yield). ^1H NMR (400 MHz, CD_2Cl_2, 293 K): $\delta = 1.10$ (d, $^3J_{HH} = 6.8$ Hz, 12H, $CH(CH_3)$, $H^{17,18,20,21}$), 1.50 (s, 6H, $C(CH_3)_2$, $H^{7,8}$), 2.55 (s, 3H, H^{25}), 3.32 (sept, $^3J_{HH} = 6.8$ Hz, 2H, $CH(CH_3)$, $H^{16,19}$), 4.30 (br s, 1H, NH), 7.09 (m, 3H, CH Ar, $H^{12,13,14}$), 7.61–7.58 (2H, $H^{2,24}$), 7.81 (t, $^3J_{HH} = 7.8$ Hz, 1H, CH Ar, H^3), 8.0 ppm (m, 1H, CH Ar, H^4); $^{13}C\{^1H\}$ NMR (100 MHz, CD_2Cl_2, 293 K): $\delta = 11.9$ (C^{25}), 23.7 ($CH(CH_3)_2$, $C^{17,18,20,21}$), 28.2 ($CH(CH_3)_2$, $C^{16,19}$), 28.7 ($C(CH_3)_2$, $C^{7,8}$), 59.1 ($C(CH_3)_2$, C^6), 116.4 (C^4), 119.8 (C^2), 122.9 ($C^{12,14}$), 124.5 (C^{13}), 136.5 (C), 137.4 (C^3), 140.2 (C), 141.8 (C^{24}), 146.7 (C), 150.2 (C), 167.8 (C), 168.0 ppm (C); elemental analysis calcd (%) for $C_{24}H_{31}N_3S$ (393.59 g mol^{-1}): C 73.24, H 7.94, N 10.68, S 8.15; found: C 73.20, H 7.93, N 10.70, S 8.17.

Synthesis of $HL^{BnTh}Me_2$ (7)

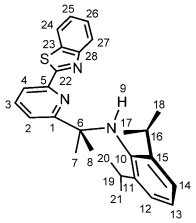

A solution of **3b** (0.50 g, 1.3 mmol) and 2-(trimethylstannyl)benzo[*d*]thiazole (**4**; 0.60 g, 2.0 mmol) in dry and degassed toluene (5 mL) was treated with a solution of $[Pd(dba)_2]$ (0.023 g, 0.04 mmol) and PPh_3 (0.081 g, 0.33 mmol) in toluene (5 mL). The reaction mixture was heated to reflux for 20 h, cooled to room temperature, and treated with water (10 mL). The resulting layers were separated; the aqueous phase was extracted with AcOEt (3×10 mL) and then dried over Na_2SO_4. The collected organic layers were evaporated under reduced pressure to give the crude product. The product was purified by recrystallization from hot MeOH, by cooling the resulting solution at −20 °C overnight to afford gray crystals (0.37 g, 63.0% yield). M.p. 133.7 °C; ^1H NMR (300 MHz, CD_2Cl_2, 293 K): $\delta = 1.11$ (d, $^3J_{HH} = 6.8$ Hz, 12H, $CH(CH_3)$, $H^{17,18,20,21}$), 1.56 (s, 6H, $C(CH_3)_2$, $H^{7,8}$), 3.32 (sept, $^3J_{HH} =$ 6.8 Hz, 2H, $CH(CH_3)$, $H^{16,19}$), 4.23 (br s, 1H, NH), 7.10 (m, 3H, CH Ar, $H^{12,13,14}$), 7.46 (m, 1H, CH BnTh, H^{26}), 7.55 (m, 1H, CH BnTh, H^{25}), 7.75 (d, $^3J_{HH} = 7.8$ Hz, 1H, CH Ar, H^2), 7.91 (t, $^3J_{HH} = 7.8$ Hz, 1H, CH Ar, H^3), 8.00 (m, 1H, CH BnTh, H^{24}), 8.11 (1H, CH Ar BnTh, H^{27}), 8.27 ppm (d, $^3J_{HH} = 7.8$ Hz, 1H, CH Ar, H^4); $^{13}C\{^1H\}$ NMR (75 MHz, CD_2Cl_2, 293 K): $\delta = 23.7$ ($CH(CH_3)_2$, $C^{17,18,20,21}$), 28.2 ($CH(CH_3)_2$, $C^{16,19}$), 28.8 ($C(CH_3)_2$, $C^{7,8}$), 59.2 ($C(CH_3)_2$, C^6), 118.0 (C^4), 121.4 (C^2), 121.9 (C^{24}), 123.0 ($C^{12,14}$), 123.4 (C^{27}), 124.5 (C^{13}), 125.4 (C^{26}), 126.1 (C^{25}), 136.3 (C), 137.5 (C^3), 140.0 (C), 146.5 (C), 149.7 (C), 154.4 (C), 168.5 (C), 170.1 ppm (C); elemental analysis calcd (%) for $C_{22}H_{27}N_3S$ (429.62 g mol^{-1}): C 75.48, H 7.27, N 9.78, S 7.46; found: C 75.40, H 7.27, N 9.83, S 7.50.

Synthesis of 8a

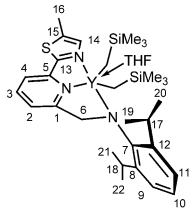

A solution of **6a** (0.277 g, 0.76 mmol) in dry and degassed toluene (3 mL) was added to a solution of $[Y(CH_2SiMe_3)_3(thf)_2]$ (0.376 g, 0.76 mmol) in dry and degassed toluene (7 mL) at 0 °C. The resulting red-purple mixture was stirred at 0 °C for 2 h, concentrated to approximately one-fourth of its initial volume, and stored at −30 °C overnight. Dark red crystals of **8a** formed. The mother liquor was decanted and the crystals were washed with cold hexane and dried in vacuum for 1 h. Complex **8a** was isolated in 74% yield (0.532 g, 0.56 mmol). ^1H NMR (400 MHz, 293 K, C_6D_6): $\delta = -0.86$ (dd, $^2J_{HH} = 10.7$, $^2J_{YH} = 2.3$ Hz, 2H, YCH_2), −0.67 (dd, $^2J_{HH} =$ 10.7, $^2J_{YH} = 2.9$ Hz, 2H, YCH_2), −0.08 (s, 18H, $SiMe_3$), 1.25 (br s, 4H, β-CH_2 thf), 1.43 (d, $^3J_{HH} = 6.9$ Hz, 6H, CH_3 *i*Pr, $H^{19,21}$), 1.52 (d, $^3J_{HH} =$ 6.9 Hz, 6H, CH_3 *i*Pr, $H^{20,22}$), 1.84 (d, $^4J_{HH} = 0.9$ Hz, 3H, CH_3, H^{16}), 3.45 (br s, 4H, α-CH_2 thf), 4.22 (sept, $^3J_{HH} = 6.9$ Hz, 2H, CH *i*Pr, $H^{17,18}$), 4.91 (s, 2H, CH_2, H^6), 6.49 (dd, $^3J_{HH} = 6.9$ Hz, $^4J_{HH} = 1.7$ Hz, 1H, CH, H^4), 6.81–6.73 (complex m, 2H, CH, $H^{2,3}$), 7.20 (dd, $^3J_{HH} = 8.3$ Hz, $^3J_{HH} =$ 6.8 Hz, 1H, CH, H^{10}), 7.28 (d, $^3J_{HH} = 7.1$ Hz, 2H, CH, $H^{9,11}$), 7.51 ppm (d, $^4J_{HH} = 0.9$ Hz, 1H, CH, H^{14}); $^{13}C\{^1H\}$ NMR (100 MHz, 293 K, C_6D_6): $\delta = 3.9$ (s, $SiMe_3$), 11.1 (s, CH_3, C^{16}), 24.9 (s, CH_3 *i*Pr, $C^{19,21}$), 25.0 (s, β-CH_2 thf), 27.0 (s, CH *i*Pr, $C^{17,18}$), 27.1 (s, CH_3 *i*Pr, $C^{20,22}$), 27.8 (d, $^1J_{YC} =$ 32.8 Hz, YCH_2), 65.7 (d, $^2J_{YC} = 2.8$ Hz, CH_2, C^6), 68.9 (br s, α-CH_2 thf), 117.4 (s, CH, C^2), 122.3 (s, CH, C^4), 123.4 (s, CH, C^{10}), 123.7 (s, CH, $C^{9,11}$), 136.4 (s, C^{15}), 138.0 (s, CH, C^3), 141.2 (s, CH, C^{14}), 147.1 (s, $C^{8,12}$), 147.5 (d, $^2J_{YC} = 0.9$ Hz, C^{13}), 151.6 (s, C^7), 164.0 (d, $^2J_{YC} = 0.8$ Hz, C^5), 168.1 ppm (d, $^2J_{YC} = 2.1$ Hz, C^1); elemental analysis calcd (%) for $C_{34}H_{56}N_3OSSi_2Y$ (699.97 g mol^{-1}): C 58.34, H 8.06, N 6.00 Y 12.70; found: C 58.70, H 8.22, N 5.97, Y 12.58.

Synthesis of 8b

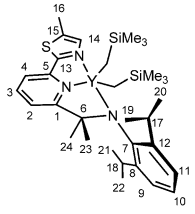

A solution of **6b** (0.330 g, 0.84 mmol) in dry and degassed toluene (3 mL) was added to a solution of $[Y(CH_2SiMe_3)_3(thf)_2]$ (0.415 g, 0.84 mmol) in dry and degassed toluene (7 mL) at 0 °C. The resulting dark red mixture was stirred at 0 °C for 2 h and then was concentrated to approximately one-fourth of its initial volume and was stored at −30 °C overnight. Dark red crystals of **8b** formed. The mother liquor was decanted and the crystals were washed with cold hexane and dried in vacuum for 1 h. Complex **8b** was isolated in 61% yield (0.336 g, 0.51 mmol). ^1H NMR (400 MHz, 293 K, C_6D_6): $\delta = -0.28$ (dd, $^2J_{HH} = 11.1$, $^2J_{YH} = 3.0$ Hz, 2H, YCH_2), −0.16 (dd, $^2J_{HH} = 11.1$, $^2J_{YH} =$ 3.1 Hz, 2H, YCH_2), 0.17 (s, 18H, $SiMe_3$), 1.26 (d, $^3J_{HH} = 6.9$ Hz, 6H, CH_3 *i*Pr, $H^{19,21}$), 1.43 (d, $^3J_{HH} = 6.9$ Hz, 6H, CH_3 *i*Pr, $H^{20,22}$), 1.51 (s, 6H, CMe_2 $H^{23,24}$), 1.60 (s, 3H, CH_3, H^{16}), 3.70 (sept, $^3J_{HH} = 6.9$ Hz, 2H, CH *i*Pr, $H^{17,18}$), 6.61 (d, $^3J_{HH} = 7.5$ Hz, 1H, CH, H^4), 6.78 (d, $^3J_{HH} = 8.0$ Hz, 1H, CH, H^2), 6.88 (t, $^3J_{HH} = 7.8$ Hz, 1H, CH, H^3), 7.21 (dd, $^3J_{HH} = 8.5$ Hz, $^3J_{HH} = 5.9$ Hz, 1H, CH, H^{10}), 7.26 (m, 2H, CH, $H^{9,11}$), 7.83 ppm (s, 1H,

CH, H[14]); $^{13}C\{^1H\}$ NMR (100 MHz, 293 K, C_6D_6): $\delta = 4.1$ (s, $SiMe_3$), 10.9 (s, CH_3, C[16]), 24.0 (s, CH_3 *i*Pr, C[19,20,21,22]), 26.9 (s, CH_3 *i*Pr, C[19,20,21,22]), 28.1 (s, CH *i*Pr, C[17,18]), 32.8 (s, $C(CH_3)_2$, C[23,24]), 35.6 (d, $^1J_{YC} = 39.2$ Hz, YCH_2), 66.1 (d, $^2J_{YC} = 2.5$ Hz, CH_2, C[6]), 117.2 (s, CH, C[4]), 121.2 (s, CH, C[2]), 123.5 (s, CH, C[9,11]), 123.9 (s, CH, C[10]), 137.5 (s, C[15]), 139.5 (s, CH, C[3]), 141.4 (s, CH, C[14]), 144.8 (s, C[7]), 146.5 (s, C[13]), 148.7 (s, C[8,12]), 168.9 (s, C[5]), 178.9 ppm (s, C[1]); $^{89}Y\{^1H\}$ NMR (19.6 MHz, C_6D_6, 293 K): $\delta = 1008$ ppm (s); elemental analysis calcd (%) for $C_{32}H_{52}N_3SSi_2Y$ (655.92 g mol^{-1}): C 58.60, H 7.99, N 6.41, Y 13.55; found: C 58.72, H 7.86, N 6.33, Y 13.31.

Synthesis of 9

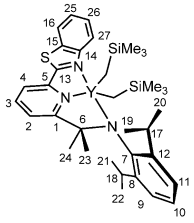

A solution of **7** (0.440 g, 1.02 mmol) in dry and degassed toluene (3 mL) was added to a solution of [Y-$(CH_2SiMe_3)_3(thf)_2$] (0.507 g, 1.02 mmol) in dry and degassed toluene (7 mL) at 0 °C. The resulting dark purple mixture was stirred at 0 °C for 2 h, and then was concentrated to approximately one-fourth of its initial volume and stored at −30 °C overnight. Dark purple crystals of **9** formed. The mother liquor was decanted and the crystals were washed with cold hexane and dried in vacuum for 1 h. Complex **9** was isolated in 75% yield (0.532 g, 0.77 mmol). ^1H NMR (400 MHz, 293 K, C_6D_6): $\delta = -0.39$ (dd, $^2J_{HH} = 11.0$, $^2J_{YH} = 2.9$ Hz, 2H, YCH_2), −0.22 (dd, $^2J_{HH} = 11.0$, $^2J_{YH} = 2.9$ Hz, 2H, YCH_2), −0.01 (s, 18H, $SiMe_3$), 1.33 (d, $^3J_{HH} = 6.8$ Hz, 6H, CH_3 *i*Pr, H[19,21]), 1.46 (d, $^3J_{HH} = 6.8$ Hz, 6H, CH_3 *i*Pr, H[20,22]), 1.51 (s, 6H, CMe_2 H[23,24]), 3.86 (sept, $^3J_{HH} = 6.8$ Hz, 2H, CH *i*Pr, H[17,18]), 6.85–6.90 (complex m, 3H, CH, H[2,3,4]), 6.93(ddd, $^3J_{HH} = 8.2$,$^3J_{HH} = 7.2$, $^3J_{HH} = 1.0$ Hz, 1H, CH, H[,26]), 7.18–7.25 (complex m, 3H, CH, H[10,25,27]), 7.30 (m, 2H, CH, H[9,11]), 8.78 ppm (d,$^3J_{HH} = 8.3$ Hz, 1H, CH, H[16]); $^{13}C\{^1H\}$ NMR (100 MHz, 293 K, C_6D_6): $\delta = 4.0$ (s, $SiMe_3$), 24.6 (s, CH_3 *i*Pr, C[19,21]), 27.1 (s, CH_3 *i*Pr, C[20,22]), 28.0 (s, CH *i*Pr, C[17,18]), 32.8 (s, $C(CH_3)_2$, C[23,24]), 34.0 (br d, $^1J_{YC} = 34.9$ Hz, YCH_2), 66.8 (d, $^2J_{YC} = 2.4$ Hz, CH_2, C[6]), 119.2 (s, CH, C[2,4]), 121.8 (s, C[16,27]), 122.6 (s, CH, C[2,4]), 123.8 (s, CH, C[9,11]), 123.9 (s, CH, C[10]), 124.5 (s, C[16,27]), 127.5 (s, C[25,26]), 128.0 (s, C[25,26]) 133.3 (s, C[15]), 139.4 (s, CH, C[3]), 145.8 (s, C[13]), 146.8 (s, C[7]), 149.0 (s, C[8,12]), 150.8 (d, $^2J_{YC} = 0.9$ Hz, C[14]), 168.5 (br s, C[5]), 179.0 ppm (br s, C[1]); elemental analysis calcd (%) for $C_{35}H_{52}N_3SSi_2Y$ (691.95 g mol^{-1}): C 60.75, H 7.57, N 6.07, Y 12.85; found: C 60.99, H 7.82, N 5.98, Y 12.67.

Synthesis of 10

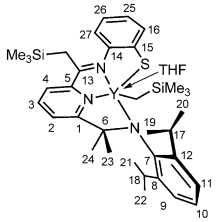

Complex **9** (0.284 g, 0.41 mmol) was dissolved in THF/hexane (1/1, 15 mL) and the solution heated at 50 °C for 6 h. The color of the reaction mixture changed from dark purple to dark red. Concentration and storage of resulting solution at −30 °C resulted in formation of red crystals of **10**. The mother liquor was decanted and the crystals were washed with cold hexane and dried in vacuum for 1 h. Complex **10** was isolated in 70% yield (0.220 g, 0.29 mmol). ^1H NMR (400 MHz, 293 K, C_6D_6): $\delta = -0.77$ (dd, $^2J_{HH} = 10.5$ Hz, $^2J_{YH} = 3.0$ Hz, 2H, YCH_2), −0.74 (dd, $^2J_{HH} = 10.5$ Hz, $^2J_{YH} = 3.0$ Hz, 2H, YCH_2), −0.21 (s, 9H, CCH_2SiMe_3), 0.06 (s, 9H, $YCH_2Si\mathit{Me}_3$), 1.14 (d, $^3J_{HH} = 6.7$ Hz, 3H, CH_3 *i*Pr, H[19]), 1.22–1.36 (complex m, 10H, CMe_2, H[23], CH_3 *i*Pr, H[21], and β-CH_2 thf), 1.44 (d, $^3J_{HH} = 6.7$ Hz, 3H, CH_3 *i*Pr, H[20]), 1.47 (d, $^3J_{HH} = 6.7$ Hz, 3H, CH_3 *i*Pr, H[22]), 1.65 (s, 3H, CMe_2 H[24]), 2.03 (d, $^2J_{HH} = 12.5$ Hz, 1H, CCH_2SiMe_3), 2.95 (d, $^2J_{HH} = 12.5$ Hz, 1H, CCH_2SiMe_3), 3.25 (br s, 4H, α-CH_2 thf), 3.78 (sept, $^3J_{HH} = 6.7$ Hz, 1H, CH *i*Pr, H[17]), 4.28 (sept, $^3J_{HH} = 6.7$ Hz, 1H, CH *i*Pr, H[18]), 6.89–7.01 (complex m, 3H, CH Ar, H[2,4,26]), 7.06–7.13 (complex m, 4H, CH, H[3,10,25,27]), 7.20 (dd,$^3J_{HH} = 7.6$ Hz, $^4J_{HH} = 1.7$ Hz,1H, CH, H[9]), 7.26 (dd, $^3J_{HH} = 7.6$ Hz, $^4J_{HH} = 1.7$ Hz, 1H, CH, H[11]), 7.83 (dd, $^3J_{HH} = 7.6$ Hz, $^4J_{HH} = 1.5$ Hz, 1H, CH, H[16]) ppm; $^{13}C\{^1H\}$ NMR (100 MHz, 293 K, C_6D_6): $\delta = -0.8$ (s, CCH_2SiMe_3), 4.1 (s, YCH_2SiMe_3), 20.8 (s, CCH_2SiMe_3), 24.5 (s, CH_3 *i*Pr, C[19,20,21,22]), 25.0 (s, β-CH_2 thf), 25.3 (s, CH_3*i*Pr, C[19,20,21,22]), 26.4 (d, $^1J_{YC} = 39.2$ Hz, YCH_2), 26.8 (s, CH_3 *i*Pr, C[19,20,21,22]), 27.2 (s, CH *i*Pr, C[17,18]), 27.9 (s, CH *i*Pr, C[17,18]), 28.4 (s, CH_3 *i*Pr, C[19,20,21,22]), 31.2 (s, $C(CH_3)_2$, C[23,24]), 32.4 (s, $C(CH_3)_2$, C[23,24]), 68.5 (br s, α-CH_2 thf), 69.6 (d, $^2J_{YC} = 2.6$ Hz, CMe_2, C[6]), 120.1 (s, CH, C[25,26]), 120.4 (s, CH, C[2,4]), 121.5 (s, CH, C[2,4]), 123.5 (s, CH, C[16,27]), 124.0 (s, CH, C[9,11]), 124.6 (s, CH, C[10]), 124.2 (s, CH, C[9,11]), 127.2 (s, C[25,26]), 135.5 (s, C[16,27]), 138.5 (s, CH, C[3]), 144.9 (s, C[14,15]), 145.0 (s, C[7]), 145.1 (s, C[14,15]), 150.2 (s, C[8,12]), 150.4 (s, C[8,12]), 153.6 (s, C[13]), 167.8 ppm (d,$^2J_{YC} = 1.0$ Hz, C[5]), 176.9 (d,$^2J_{YC} = 1.3$ Hz, C[1]); elemental analysis calcd (%) for $C_{39}H_{60}N_3OSSi_2Y$ (764.06 g mol^{-1}): C 61.31, H 7.92, N 5.50, Y 11.64; found: C 61.53, H 7.90, N 5.61, Y 11.35.

General procedure for intramolecular hydroamination of amino alkenes

Two different cyclization protocols were explored, depending on the employed catalyst system. Both procedures were set up under an inert atmosphere in a N_2-filled dry box. The conversion of each reaction was monitored by NMR spectroscopy (by a comparative integration of selected proton signals on the substrate and their corresponding protons on the cyclization product) and gas chromatography (by integration of the reagent and product signals). Selected experiments were additionally monitored by ^1H NMR spectroscopy with ferrocene as internal standard (0.2 mL of a stock 0.17 M ferrocene solution in [D_8]toluene). The internal standard was used to measure the substrate conversion and confirm the appropriate reaction mass balance. In all cases, the reaction mass balance was confirmed at the limit of the NMR spectrometer experimental error (^1H NMR acquisition parameters: acquisition time (aq.): 5 s; d1: 8 s; scan number (ns): 32).

Procedure A: catalysis by neutral dialkyl yttrium complexes: In a typical procedure, a solution of the selected dialkyl complex (1.05–5 μmol%) in dry and degassed toluene (1.5 mL) was slowly added to a two-necked 10 mL round bottom flask previously charged with a preheated, dry, and degassed solution of the desired amino alkene (0.21 mmol) and ferrocene as internal standard (0.2 mL of a stock 0.17 M ferrocene solution in toluene) in toluene (1 mL). The system was then stirred at the desired temperature and the course of the reaction was periodically monitored by analyzing a sample of the mixture by GC-MS until completeness or at fixed times.

Procedure B: catalysis by cationic monoalkyl yttrium complexes: In a typical procedure, a toluene solution (0.5 mL) of the activator $Ph_3C^+[B(C_6F_5)_4]^-$ was slowly added to a solution of the dialkyl complex (1.05–5 μmol%) in toluene (1 mL) at RT. The solution was rapidly stirred and transferred to a two-necked 10 mL round-bottom flask previously charged with a preheated, dry, and degassed solution of the desired amino alkene (0.21 mmol) and ferrocene as internal standard (0.2 mL of a stock 0.17 M ferrocene solution in toluene) in toluene (1 mL). The system was then stirred at the desired temperature and the course of the reaction was periodically monitored by analyzing a sample of the mixture by GC-MS until completeness or at fixed times.

Generation of cationic monoalkyl complexes by treatment of the dialkyl precursors with $Ph_3C^+[B(C_6F_5)_4]^-$ in situ

The generation of the cationic monoalkyl catalysts was monitored by ^{1}H NMR spectroscopy on the most soluble system in [D_6]benzene. Indeed, for all cationic monoalkyl systems a dark red rubbery precipitate started to form within a few minutes, and the most soluble one was that resulting from activation of **9** (**9**$^+$). Although poorly soluble in aromatic hydrocarbons, the activated complexes are stable as precipitates for days with no apparent decomposition. Polar aromatics such as mono- or dihalobenzenes (halo = Cl, Br) increase the solubility of the complex while causing progressive catalyst degradation with the generation of untreatable dark-brown semisolid materials. To improve the solubility of the activated complex **9**$^+$ and thus allow its characterization by ^{1}H NMR spectroscopy, $Ph_3C^+[B(C_6F_5)_4]^-$ (1 equiv) was dissolved in C_6D_5Br (0.2 mL) and added in one portion to a dry and degassed dark purple solution of dialkyl complex **9** (0.021 mmol, 1 equiv) in [D_6]benzene (0.5 mL). The resulting mixture was placed in a J. Young NMR tube and immediately used for recording the ^{1}H NMR spectra (see Supporting Information). Quantitative conversion of **9** to cationic monoalkyl complex **9**$^+$ was observed in the ^{1}H NMR spectrum by the concomitant appearance of signals attributed to the formation of $Me_3SiCH_2CPh_3$ (73.2% as two isomers in a ca. 2:1 ratio)[39] and Ph_3CH (26.8%)[39] as side products. ^{1}H NMR (400 MHz, C_6D_6/C_6D_5Br, 293 K, selected data): $\delta = 0.46$ (br s, 2H, YCH_2SiMe_3), −0.12 (s, $Me_3SiCH_2CPh_3$ of isomer A), −0.04 (s, 9H, YCH_2SiMe_3), 0.10 (s, $Me_3SiCH_2CPh_3$ of isomer B), 1.20 (m, 12H, $CH(CH_3)_2$), 1.34 (s, 6H, CH_3), 2.03 (s, $Me_3SiCH_2CPh_3$ of isomer B), 2.16 (s, $Me_3SiCH_2CPh_3$ of isomer A), 3.16 (m, 2H, $CH(CH_3)_2$), 5.52 ppm (s, Ph_3CH).

Computational details

DFT calculations are performed by using the Gaussian 09 program suite (revision A.02).[40] Model structures were optimized with the M06 functional[41] by using the SDD/D95 pseudopotential and related basis set[42] on the yttrium, silicon, and sulfur atoms plus a 6-31G* basis set on all other atoms. An extra d-type polarization function for Si/S and an extra f-type function for yttrium were added to the standard set.[43] Gibbs free-energy calculations to determine relative thermodynamic stabilities for both thiazole reduction and ring-opening reactions were carried out on model systems. An initial geometry guess for the optimizations was obtained from the XRD structure of **8b** by replacing the 2,6-*i*Pr(C_6H_3) substituent of the amido fragment and the methyl groups of the CH_2SiMe_3 substituents with H atoms, in order to reach a satisfactory compromise between accuracy of the model system and short computation times. The simplified models are outlined in Scheme 4. Solvent effects were evaluated by discrete + continuum modeling of the reaction medium. One thf molecule coordinated to the metal center was added for discrete solvent modeling, so that the alternative solvate complex (Scheme 4, **9b**^{thf}) was also considered, while bulk solvent effects (THF/*n*-hexane 1/1) were expressed through the SMD Continuum Model[44] with the same basis set as used for the gas-phase optimizations and assuming a dielectric constant equal to the mean value of those of the pure solvents ($\varepsilon_{solv} = (\varepsilon_{THF} + \varepsilon_{hex})/2 = 4.67$). Gibbs free energy in solution was calculated according to the simplified Equation (1).

$$G_{solv} = G_{gas} + (E_{solv} - E_{gas}) \quad (1)$$

Acknowledgements

The authors thank the Russian Foundation for Basic Research (Project 12-03-93109-NTSNIL a) and the Groupe de Recherche International (GDRI) "Homogeneous Catalysis for Sustainable Development" for support to this work.

Keywords: hydroamination · N ligands · ring opening · tridentate ligands · yttrium

[1] a) S. A. Cotton, *Coord. Chem. Rev.* **1997**, *160*, 93 – 127; b) N. Marques, A. Sella, J. Takats, *Chem. Rev.* **2002**, *102*, 2137 – 2160; c) M. Zimmermann, R. Anwander, *Chem. Rev.* **2010**, *110*, 6194 – 6259.

[2] a) P. L. Watson, *J. Chem. Soc. Chem. Commun.* **1983**, 276 – 277; b) P. L. Watson, G. W. Parshall, *Acc. Chem. Res.* **1985**, *18*, 51 – 56; c) J. E. Bercaw, *Pure Appl. Chem.* **1990**, *62*, 1151 – 1154; d) M. E. Thompson, S. M. Baxter, A. R. Bulls, B. J. Burger, M. C. Nolan, B. D. Santarsiero, W. P. Schaefer, J. E. Bercaw, *J. Am. Chem. Soc.* **1987**, *109*, 203 – 219; e) M. Booij, B.-J. Deelman, R. Duchateau, D. S. Postma, A. Mettsma, J. H. Teuben, *Organometallics* **1993**, *12*, 3531 – 3540; f) K. H. den Haan, Y. Wielstra, J. H. Teuben, *Organometallics* **1987**, *6*, 2053 – 2060; g) F.-G. Fontaine, T. D. Tilley, *Organometallics* **2005**, *24*, 4340 – 4342.

[3] A. D. Sadow, T. D. Tilley, *J. Am. Chem. Soc.* **2003**, *125*, 7971 – 7977.

[4] a) Z. Hou, Y. Wakatsuki, *Coord. Chem. Rev.* **2002**, *231*, 1 – 22; b) Y. Nakayama, H. Yasuda, *J. Organomet. Chem.* **2004**, *689*, 4489 – 4498; c) J. Gromada, J.-F. Carpentier, A. Mortreux, *Coord. Chem. Rev.* **2004**, *248*, 397 – 410.

[5] a) G. Jeske, H. Lauke, H. Mauermann, P. N. Swepston, H. Schumann, T. J. Marks, *J. Am. Chem. Soc.* **1985**, *107*, 8091 – 8103; b) G. Jeske, L. E. Schock, P. N. Swepston, H. Schumann, T. J. Marks, *J. Am. Chem. Soc.* **1985**, *107*, 8103 – 8110.

[6] G. A. Molander, J. A. C. Romero, *Chem. Rev.* **2002**, *102*, 2161 – 2186.

[7] a) S. Hong, T. J. Marks, *Acc. Chem. Res.* **2004**, *37*, 673 – 686; b) T. E. Müller, K. C. Hultzsch, M. Yus, F. Foubelo, M. Tada, *Chem. Rev.* **2008**, *108*, 3795 – 3892; c) F. Pohlki, S. Doye, *Chem. Soc. Rev.* **2003**, *32*, 104 – 114; d) J. Hannedouche, E. Schulz, *Chem. Eur. J.* **2013**, *19*, 4972 – 4985.

[8] a) K. N. Harrison, T. J. Marks, *J. Am. Chem. Soc.* **1992**, *114*, 9220 – 9221; b) E. A. Bijpost, R. Duchateau, J. H. Teuben, *J. Mol. Catal. A* **1995**, *95*, 121 – 128.

[9] a) S. Arndt, J. Okuda, *Chem. Rev.* **2002**, *102*, 1953 – 1976; b) A. A. Trifonov in *Olefin Upgrading Catalysis by Nitrogen-based Metal Complexes, Vol. 35* (Eds.: G. Giambastiani, J. Cámpora), Springer, **2011**, pp. 119 – 152; c) S. Arndt, J. Okuda, *Adv. Synth. Catal.* **2005**, *347*, 339 – 354; d) Z. Hou, Y. Luo, X. Li, *J. Organomet. Chem.* **2006**, *691*, 3114 – 3121; e) P. M. Zeimentz, S. Arndt, B. R. Elvidge, J. Okuda, *Chem. Rev.* **2006**, *106*, 2404 – 2433; f) M. Zimmermann, K. W. Törnroos, R. Anwander, *Angew. Chem.* **2008**, *120*, 787 – 790; *Angew. Chem. Int. Ed.* **2008**, *47*, 775 – 778; g) D. Li, S. Li, D. Cui, X. Zhang, *Organometallics* **2010**, *29*, 2186 – 2193; h) K. Lv, D. Cui, *Organometallics* **2010**, *29*, 2987 – 2993; i) L. Wang, D. Cui, Z. Hou, W. Li, Y. Li, *Organometallics* **2011**, *30*, 760 – 767; j) Y. Luo, S. Fan, J. Yang, J. Fang, P. Xu, *Dalton Trans.* **2011**, *40*, 3053 – 3059; k) D. Robert, D. Abinet, T. P. Spaniol, J. Okuda, *Chem. Eur. J.* **2009**, *15*, 11937 – 11947; l) G. Du, Y. Wei, L. Ai, Y. Chen, Q. Xu, X. Liu, S. Zhang, Z. Hou, X. Li, *Organometallics* **2011**, *30*, 160 – 170; m) S. Li, D. Cui, D. Li, Z. Hou, *Organometallics* **2009**, *28*, 4814 – 4822; n) L. Li, C. Wu, D. Liu, S. Li, D. Cui, *Organometallics* **2013**, *32*, 3203 – 3209; o) Y. Pan, T. Xu, G.-W. Yang, K. Jin, X.-B. Lu, *Inorg. Chem.* **2013**, *52*, 2802 – 2808; p) W. Rong, D. Liu, H. Zuo, Y. Pan, Z. Jian, S. Li, D. Cui, *Organometallics* **2013**, *32*, 1166 – 1175; q) L. Wang, D. Liu, D. Cui, *Organometallics* **2012**, *31*, 6014 – 6021.

[10] a) F. T. Edelmann, D. M. M. Freckmann, H. Schumann, *Chem. Rev.* **2002**, *102*, 1851 – 1896; b) W. E. Piers, D. J. H. Emslie, *Coord. Chem. Rev.* **2002**, *233 – 234*, 131 – 155; c) A. A. Trifonov, *Russ. Chem. Rev.* **2007**, *76*, 1051 – 1072.

[11] a) D. M. Lyubov, C. Döring, G. K. Fukin, A. V. Cherkasov, A. S. Shavyrin, R. Kempe, A. A. Trifonov, *Organometallics* **2008**, *27*, 2905 – 2907; b) D. M. Lyubov, C. Döring, S. Y. Ketkov, R. Kempe, A. A. Trifonov, *Chem. Eur. J.* **2011**, *17*, 3824 – 3826.

[12] a) D. M. Lyubov, G. K. Fukin, A. V. Cherkasov, A. S. Shavyrin, A. A. Trifonov, L. Luconi, C. Bianchini, A. Meli, G. Giambastiani, *Organometallics*

2009, *28*, 1227 – 1232; b) L. Luconi, D. M. Lyubov, C. Bianchini, A. Rossin, C. Faggi, G. K. Fukin, A. V. Cherkasov, A. S. Shavyrin, A. A. Trifonov, G. Giambastiani, *Eur. J. Inorg. Chem.* **2010**, 608 – 620; c) A. A. Karpov, A. V. Cherkasov, G. K. Fukin, A. S. Shavyrin, L. Luconi, G. Giambastiani, A. A. Trifonov, *Organometallics* **2013**, *32*, 2379 – 2388.

[13] M. F. Lappert, R. J. Pearce, *J. Chem. Soc. Chem. Commun.* **1973**, 126 – 126.

[14] L. Luconi, A. Rossin, A. Motta, G. Tuci, G. Giambastiani, *Chem. Eur. J.* **2013**, *19*, 4906 – 4921; and references therein.

[15] For a general procedure for the preparation of the trimethylstannyl derivatives, see: K. C. Molloy, P. C. Waterfield, M. F. Mahon, *J. Organomet. Chem.* **1989**, *365*, 61 – 73.

[16] 5-Methyl-2-(trimethylstannyl)thiazole (**5**) was prepared by using the literature procedure reported for the preparation of 2-(trimethylstannyl)-benzothiazole (**4**).[15]

[17] a) C. Bianchini, G. Giambastiani, G. Mantovani, A. Meli, D. Mimeau, *J. Organomet. Chem.* **2004**, *689*, 1356 – 1361; b) P. Barbaro, C. Bianchini, G. Giambastiani, I. Guerrero Rios, A. Meli, W. Oberhauser, A. M. Segarra, L. Sorace, A. Toti, *Organometallics* **2007**, *26*, 4639 – 4651; c) C. Bianchini, G. Giambastiani, I. Guerrero Rios, A. Meli, W. Oberhauser, L. Sorace, A. Toti, *Organometallics* **2007**, *26*, 5066 – 5078.

[18] M. M. Salter, J. Kobayashi, Y. Shimizu, S. Kobayashi, *Org. Lett.* **2006**, *8*, 3533 – 3536.

[19] a) S. Bambirra, D. van Leusen, A. Meetsma, B. Hessen, J. H. Teuben, *Chem. Commun.* **2001**, 637 – 638; b) Y. Luo, X. Wang, J. Chen, C. Luo, Y. Zhang, Y. Yao, *J. Organomet. Chem.* **2009**, *694*, 1289 – 1296; c) V. Yu. Rad'kov, G. G. Skvortsov, D. M. Lyubov, A. V. Cherkasov, G. K. Fukin, A. S. Shavyrin, D. Cui, A. A. Trifonov, *Eur. J. Inorg. Chem.* **2012**, 2289 – 2297; d) M. Ohashi, M. Konkol, I. Del Rosal, R. Poteau, L. Maron, J. Okuda, *J. Am. Chem. Soc.* **2008**, *130*, 6920 – 6921; e) J. Cheng, K. Saliu, G. Y. Kiel, M. J. Ferguson, R. McDonald, J. Takats, *Angew. Chem.* **2008**, *120*, 4988 – 4991; *Angew. Chem. Int. Ed.* **2008**, *47*, 4910 – 4913; f) S. Bambirra, S. J. Boot, D. van Leusen, A. Meetsma, B. Hessen, *Organometallics* **2004**, *23*, 1891 – 1898; g) D. M. Lyubov, G. K. Fukin, A. A. Trifonov, *Inorg. Chem.* **2007**, *46*, 11450 – 11456; h) A. A. Trifonov, D. M. Lyubov, G. K. Fukin, E. V. Baranov, Yu. A. Kurskii, *Organometallics* **2006**, *25*, 3935 – 3942.

[20] a) S. Bambirra, A. Meetsma, B. Hessen, *Organometallics* **2006**, *25*, 3486 – 3495; b) W. Gao, D. Cui, X. Liu, Y. Zhang, Y. Mu, *Organometallics* **2008**, *27*, 5889 – 5893.

[21] The calculated trigonality factor τ for **8b** is 0.24; see also: A. W. Addison, T. N. Rao, J. Reedijk, J. van Rijn, G. C. Verschoor, *J. Chem. Soc. Dalton Trans.* **1984**, 1349.

[22] a) A. P. Purdy, A. D. Berry, C. F. George, *Inorg. Chem.* **1997**, *36*, 3370 – 3375; b) Z. Zhang, L. Zhang, Y. Li, L. Hong, Z. Chen, X. Zhou, *Inorg. Chem.* **2010**, *49*, 5715 – 5722.

[23] For covalent Y–N bonds in six-coordinate complexes, see: a) K. C. Hultzsch, P. Voth, K. Beckerle, T. P. Spaniol, J. Okuda, *Organometallics* **2000**, *19*, 228 – 243; b) C.-X. Cai, L. Toupet, C. W. Lehmann, J.-F. Carpentier, *J. Organomet. Chem.* **2003**, *683*, 131 – 136; c) D. Wang, D. Cui, W. Miao, S. Li, B. Huang, *Dalton Trans.* **2007**, 4576 – 4581; d) X. Liu, X. Shang, T. Tang, N. Hu, F. Pei, D. Cui, X. Chen, X. Jing, *Organometallics* **2007**, *26*, 2747 – 2757; e) G. G. Skvortsov, G. K. Fukin, A. A. Trifonov, A. Noor, C. Döring, R. Kempe, *Organometallics* **2007**, *26*, 5770 – 5773; f) W. Miao, S. Li, D. Cui, B. Huang, *J. Organomet. Chem.* **2007**, *692*, 3823 – 3834; g) Y. Luo, W. Li, D. Lin, Y. Yao, Y. Zhang, Q. Shen, *Organometallics* **2010**, *29*, 3507 – 3514.

[24] For Y–N coordination bonds in six-coordinate complexes, see: a) S. Jie, P. L. Diaconescu, *Organometallics* **2010**, *29*, 1222 – 1230; b) M. Zimmermann, F. Estler, E. Herdtweck, K. W. Törnroos, R. Anwander, *Organometallics* **2007**, *26*, 6029 – 6041; c) M. E. G. Skinner, P. Mountford, *J. Chem. Soc. Dalton Trans.* **2002**, 1694 – 1703; d) T. K. Panda, D. Petrovic, T. Bannenberg, C. G. Hrib, P. G. Jones, M. Tamm, *Inorg. Chim. Acta* **2008**, *361*, 2236 – 2242.

[25] F. H. Allen, O. Kennard, D. G. Watson, L. Brammer, A. G. Orpen, R. Taylor, *J. Chem. Soc. Perkin Trans. 2* **1987**, S1 – S19.

[26] a) S. D. Gray, K. J. Weller, M. A. Bruck, P. M. Briggs, D. E. Wigley, *J. Am. Chem. Soc.* **1995**, *117*, 10678 – 10693; b) K. J. Weller, S. D. Gray, P. M. Briggs, D. E. Wigley, *Organometallics* **1995**, *14*, 5588 – 5597; c) H. Sugiyama, G. Aharonian, S. Gambarotta, G. P. A. Yap, P. H. M. Budzelaar, *J. Am. Chem. Soc.* **2002**, *124*, 12268 – 12274; d) J. Scott, S. Gambarotta, I. Korobkov, P. H. M. Budzelaar, *J. Am. Chem. Soc.* **2005**, *127*, 13019 – 13029; e) G. Giambastiani, L. Luconi, R. L. Kuhlman, P. D. Hustad in *Olefin Upgrading Catalysis by Nitrogen-based Metal Complexes I* (Eds.: G. Giambastiani, J. Campora) Springer, London, **2011**, pp. 197 – 282; and references therein.

[27] a) T. M. Cameron, J. C. Gordon, B. L. Scott, W. Tumas, *Chem. Commun.* **2004**, 1398 – 1399.

[28] K. C. Jantunen, B. L. Scott, P. J. Hay, J. C. Gordon, J. L. Kiplinger, *J. Am. Chem. Soc.* **2006**, *128*, 6322 – 6323.

[29] A dielectric constant equal to the mean value of those of the pure solvents was considered ($\varepsilon_{solv} = (\varepsilon_{THF} + \varepsilon_{hex})/2 = 4.67$).

[30] G. Giambastiani, A. Trifonov, A. Rossin, unpublished results.

[31] A. Z. Voskoboynikov, I. N. Parshina, A. K. Shestakova, K. P. Butin, I. P. Beletskaya, L. G. Kuz'mina, J. A. K. Howard, *Organometallics* **1997**, *16*, 4041 – 4055.

[32] J. Cheng, M. J. Ferguson, J. Takats, *J. Am. Chem. Soc.* **2010**, *132*, 2 – 3.

[33] a) M. R. Gagne, T. J. Marks, *J. Am. Chem. Soc.* **1989**, *111*, 4108 – 4109; b) M. R. Gagne, S. P. Nolan, T. J. Marks, *Organometallics* **1990**, *9*, 1716 – 1718; c) M. R. Gagne, C. L. Stern, T. J. Marks, *J. Am. Chem. Soc.* **1992**, *114*, 275 – 294; d) M. R. Gagne, L. Brard, V. P. Conticello, M. A. Giardello, C. L. Stern, T. J. Marks, *Organometallics* **1992**, *11*, 2003 – 2005.

[34] For a selection of rare earth metal catalyzed (enantioselective) intra- and intermolecular hydroamination reactions, see: a) Y. Li, T. J. Marks, *Organometallics* **1996**, *15*, 3770 – 3772; b) J. S. Ryu, G. Y. Li, T. J. Marks, *J. Am. Chem. Soc.* **2003**, *125*, 12584 – 12605; c) S. Hong, S. Tian, M. V. Metz, T. J. Marks, *J. Am. Chem. Soc.* **2003**, *125*, 14768 – 14783; d) P. N. O'Shaughnessy, P. D. Knight, C. Morton, K. M. Gillespie, P. Scott, *Chem. Commun.* **2003**, 1770 – 1771; e) J. Y. Kim, T. Livinghouse, *Org. Lett.* **2005**, *7*, 1737 – 1739; f) N. Meyer, A. Zulys, P. W. Roesky, *Organometallics* **2006**, *25*, 4179 – 4182; g) D. V. Gribkov, K. C. Hultzsch, F. Hampel, *J. Am. Chem. Soc.* **2006**, *128*, 3748 – 3759; h) I. Aillaud, J. Collin, C. Duhayon, R. Guillot, D. Lyubov, E. Schulz, A. Trifonov, *Chem-Eur. J.* **2008**, *14*, 2189 – 2200; i) G. Zi, L. Xiang, H. Song, *Organometallics* **2008**, *27*, 1242 – 1246; j) Y. Chapurina, J. Hannedouche, J. Collin, R. Guillot, E. Schulz, A. Trifonov, *Chem. Commun.* **2010**, *46*, 6918 – 6920; k) A. L. Reznichenko, H. N. Nguyen, K. C. Hultzsch, *Angew. Chem.* **2010**, *122*, 9168 – 9171; *Angew. Chem. Int. Ed.* **2010**, *49*, 8984 – 8987; l) Y. Chapurina, H. Ibrahim, R. Guillot, E. Kolodziej, J. Collin, A. Trifonov, E. Schulz, J. Hannedouche, *J. Org. Chem.* **2011**, *76*, 10163 – 10172; m) D. V. Vitanova, F. Hampel, K. C. Hultzsch, *J. Organomet. Chem.* **2011**, *696*, 321 – 330; n) P. Benndorf, J. Jenter, L. Zielke, P. W. Roesky, *Chem. Commun.* **2011**, *47*, 2574 – 2576; o) H. M. Lovick, D. K. An, T. S. Livinghouse, *Dalton Trans.* **2011**, *40*, 7697 – 7700.

[35] A. Motta, G. Lanza, I. L. Fragalà, T. J. Marks, *Organometallics* **2004**, *23*, 4097 – 4104.

[36] S. Bambirra, H. Tsurugi, D. van Leusen, B. Hessen, *Dalton Trans.* **2006**, 1157 – 1161.

[37] F. Lauterwasser, P. G. Hayes, S. Bräse, W. E. Piers, L. L. Schafer, *Organometallics* **2004**, *23*, 2234 – 2237.

[38] L. J. Farrugia, *J. Appl. Crystallogr.* **1997**, *30*, 565.

[39] P. D. Bolton, E. Clot, N. Adams, S. R. Dubberley, A. R. Cowley, P. Mountford, *Organometallics* **2006**, *25*, 2806 – 2825.

[40] Frisch M. J. et al., *Gaussian09*, Revision A.02, Gaussian Inc., Wallingford CT, **2009**.

[41] Y. Zhao, D. G. Truhlar, *Theor. Chem. Acc.* **2008**, *120*, 215 – 241.

[42] a) D. Andrae, U. Haeuessermann, M. Dolg, H. Stoll, H. Preuss, *Theor. Chim. Acta* **1990**, *77*, 123 – 141; b) T. H. Dunning Jr., P. J. Hay, in *Modern Theoretical Chemistry, Vol. 3* (Ed.: H. F. Schaefer, III), Plenum, New York, **1976**, pp. 1 – 28.

[43] a) A. Höllwarth, M. Böhme, S. Dapprich, A. W. Ehlers, A. Gobbi, V. Jonas, K. F. Köhler, R. Stegmann, A. Veldkamp, G. Frenking, *Chem. Phys. Lett.* **1993**, *208*, 237 – 240; b) A. W. Ehlers, M. Böhme, S. Dapprich, A. Gobbi, A. Höllwarth, V. Jonas, K. F. Köhler, R. Stegmann, A. Veldkamp, G. Frenking, *Chem. Phys. Lett.* **1993**, *208*, 111 – 114.

[44] A. V. Marenich, C. J. Cramer, D. G. Truhlar, *J. Phys. Chem. B* **2009**, *113*, 6378 – 6396.

Received: October 2, 2013
Published online on February 24, 2014